Cleaner Energy Systems 13 (2026) 100229

Contents lists available at ScienceDirect

Cleaner Energy Systems

journal homepage: www.elsevier.com/locate/cles

Hydrogen impact on gas turbine operating flexibility in simple and combined cycle mode

Matteo Cappellini, Chiara Castagna, Silvia Ravelli *

Department of Engineering and Applied Sciences, University of Bergamo, 24044 Dalmine, Italy

ARTICLE INFO

Keywords:
Gas turbine
Simple cycle
Combined cycle
Hydrogen
Peaking
Load-following

ABSTRACT

This study addresses two topical issues: carbon-free power production, on the one hand, and secure and reliable energy supply on the other hand. Undeniably, to integrate increasing shares of renewables into sustainable and competitive electricity systems, "capacity mechanisms", i.e., a range of solutions aimed at ensuring adequate power capacity, are needed. Clean, dispatchable power generation is one such solution. Specifically, gas turbines fed by green fuels such as hydrogen can be scheduled to provide power when the contribution from solar and wind sources is not enough to meet the demand or in challenging situations, even for a few hours per year. With the idea of retrofitting existing gas turbine (GT) plants to hydrogen combustion, a thermodynamic model was developed by means of Thermoflex® software in a dual context: peaking, with a small, simple-cycle (SC) GT or "load-following", with a large size combined cycle (CC) with 1 × 1 configuration. In both cases, *ad hoc* control strategies were implemented to increase thermal efficiency (η) at partial load. Simulations were run on an hourly basis to meet the prescribed load profiles at representative locations, for two typical hot and cold days: computations were carried out assuming 100% hydrogen as fuel, for comparison against conventional natural gas (NG), given the same GT output requirement and environmental condition. This study's novelty stems from these constraints.

The results show that replacing NG with hydrogen combines obvious decarbonization with increases in net power (P_n) and net efficiency (η_n), the magnitude of which depends on the off-design control strategy, which in turn is a function of the GT operating environment. Overall, the largest increase in η_n was quantified at about 0.6 percentage points (pp). Furthermore, the combustor shifted towards leaner conditions so that the maximum cycle temperature does not exceed that with the conventional fuel.

1. Introduction

There has been a considerable surge in interest in hydrogen as carbon-free fuel in recent years, propelled by the pressing need to address global warming and the projected escalation in worldwide demand for electricity (4 % annually through 2027), driven by use for air conditioning, electrification and data centers (IEA, 2025). Although the current use of hydrogen remains concentrated in industry and refining, new applications in heavy industry, transport and power generation are receiving growing attention. With regard to the latter, models of fuel cells, internal combustion engines, and gas turbines that can run on hydrogen-rich gases or even pure hydrogen are available on the market (IEA, 2023). Hydrogen capacity for power generation is expected to grow by 65 % percent by 2030 (IEA, 2024). The majority of the announced projects (approximately two-thirds) is focused on the utilization of hydrogen in open-cycle or combined-cycle gas turbines. This involves demonstrations of existing GT units adapted to run on hydrogen co-firing shares and the design of new GT models fed by 100 % H_2 by the end of the decade.

1.1. Hydrogen capability of gas turbines

As a matter of fact, GT hydrogen capability is extending year by year, as shown by recent literature. The maximum hydrogen content varies depending on the GT model: 60 % vol for SGT5–4000F (Blaette et al., 2023; Blätte et al., 2024) and 7EA (Demougeot et al., 2024); 44 % vol for GE LM6000 (Steele et al., 2023); 20.9 % vol for M501G (Harper et al., 2023). The SGT6–6000 G model from Siemens Energy proved its reliability at baseload with a hydrogen blending percentage of 38.8 % vol at the Constellation Hillabee power plant, as confirmed by tests that left the existing architecture unchanged (Harper et al., 2025). Similarly,

* Corresponding author at: Department of Engineering and Applied Sciences, University of Bergamo, Marconi St. 5, 24044 Dalmine, Italy.
E-mail address: silvia.ravelli@unibg.it (S. Ravelli).

https://doi.org/10.1016/j.cles.2025.100229
Received 4 May 2025; Received in revised form 14 September 2025; Accepted 23 December 2025
Available online 26 December 2025

Nomenclature

c	specific heat, J/kg·K
CC	combined cycle
COT	compressor outlet temperature, K
DLE	dry low-emission
DLN	dry low-NOx
ETN	European Turbine Network
GT	gas turbine
HP	high pressure
HRSG	heat recovery steam generator
IGV	inlet guide vane
LCOE	levelized cost of electricity
LHV	lower heating value, J/kg
LP	low pressure
m	mass flow rate, kg/s
M	Mach number
MP	middle pressure
n	rotational speed (RPM)
NG	natural gas
P	power, W
p	pressure, bar
pp	percentage points
R	gas constant, J/mol·K
SC	simple cycle
ST	steam turbine
T	temperature, K
TIT	turbine inlet temperature, K
TOT	turbine outlet temperature, K
UD	user-defined
vol	volume
β	pressure ratio, -
Φ	equivalence ratio, -
γ	specific heat ratio, -
η	thermal efficiency, %

Subscript

a	air
amb	ambient
ax	axial
c	coolant
f	fuel
g	gross
i	inlet
n	net
Rk	Rankine
st	stoichiometric
tg	tangential
y	polytropic

stable and safe operation up to 25 % vol H_2 was observed for the Siemens SGT-600 in the port of Antwerp (Belgium), without any hardware modification (Laget et al., 2022). Horikawa et al. (2022) documented in detail the operation of an M1A-17 GT fed by pure hydrogen at the cogeneration power plant in Kobe city (Japan). Other demonstration cases reported in the media have been listed in Table 1, with indication of location, GT characteristics, and H_2 share: they span the three-year period from 2024 to 2026. Furthermore, the latest experimental campaigns include partial load operation, as in the case of SGT-600 (Berg and Magnusson, 2023) and SGT-400 (Parsania et al., 2024). The former was tested at all loads with up to 60 % vol H_2 in the fuel. For the latter, detailed experience was gained as part of the HYFLEXPOWER project: the load was reduced by up to 10 %, with a volume fraction of H_2 between 60 % and 100 %.

The distinguishing factor is generally attributable to the combustion technology adopted, as hydrogen differs from NG in many characteristics (NETL, 2022), including:

- the flame speed is roughly an order of magnitude faster, with the risk of flashback;
- the energy density by volume is more than three times lower, so the injection nozzle diameter must be enlarged to allow more fuel into the chamber, for the same amount of fuel energy input;
- the density is lower, so there is a propensity for leakage;
- the flame temperature is higher, leading to increased metal temperatures, potentially higher (thermal) NO_x emissions and changes to combustor thermo-acoustics;
- with a wider flammability limit and much lower ignition energy, an explosive mixture may occur in the GT package;
- the water vapor content in the combustion products is higher, leading to an increase in the heat transfer coefficient of the gas. This, in turn, results in higher temperatures of the metal blades in the first turbine stages, which are subjected to the largest heat load.

Table 1
Hydrogen fueling projects in GT plants.

Location	Company	GT model/size	%H_2 vol
Daesan (South Korea)	Hanwha	80 MW	100
Takasago (Japan)	Mitsubishi	M501JAC	30
DeBary (Florida, US)	GE Vernova	7E	100
North Lincolnshire (UK)	Siemens Energy	SGT5–9000HL	50
Whyalla (Australia)	GE Vernova	LM6000(VELOX)	100
Brigalow (Australia)	GE Vernova	LM2500XPRESS	35
Brentwood (California, US)	GE Vernova	LM6000 SAC	44
Cologne (Germany)	Ansaldo Energia	GT36 H	70
Plaquemine (Louisiana, US)	GE Vernova	7HA03	50

In addition, material-related problems involve oxidation/corrosion of base alloys and spallation of thermal barrier coatings, leading to consequent trade-offs between component durability and performance (Stefan et al., 2022).

1.2. Hydrogen challenges and "readiness"

It is beyond doubt that the main challenge lies in the design of the combustor to admit fuels with such different behavior. Diffusion flame combustors, which are characterized by nearly stoichiometric fuel/air mixture regions in the primary combustion zone, are 100 % H_2 ready but an inert diluent, such as nitrogen and water vapor, is required to reduce NO_x emissions. Nevertheless, high volumes of diluent can disrupt the matching between compressor and turbine that has been designed for NG. Loss of surge margins may necessitate turbine or compressor modifications, such as opening the turbine stage first nozzle throat area and adjusting the compressor inlet guide vane (IGV) schedule. All this causes a significant decrease in the plant efficiency (Gazzani et al., 2014).

Therefore, much attention has been paid to lean premixed combustion systems available in most GT engines, in which NO_x mitigation is achieved by diluting the fuel with air before entering the combustion zone. But hydrogen brings additional challenges to premixing, particularly with regard to flashback and flame holding. In fact, dry low-NO_x (DLN) and dry low-emission (DLE) combustors designed for NG are being adapted to hydrogen characteristics according to different approaches: aerodynamically stabilized combustion; self-ignition combustion; staged combustion; micro-mixing (Cecere et al., 2023).

On the one hand, moderate hydrogen content is generally recommended in retrofit solutions to maintain the same level of NO_x emission as NG (so as to not compromise existing permits) while preserving the whole hot-gas-path. Obviously, some major modifications are needed in existing NG plants to admit hydrogen, such as replacing the combustor, modifying the fuel system, and adding hydrogen gas systems as well as monitoring and control equipment (Pigon et al., 2023; Zhou et al., 2024). On the other hand, commercial-grade 100 % hydrogen engines, with similar or better NO_x emission performance than NG engines, are projected to be produced around 2030, according to publicly announced forecasts (Kytömaa et al., 2024).

It must be said that the most stringent limitation preventing full-scale testing for a long time is identified in the availability and supply of hydrogen. On-site production/storage of hydrogen covered only a few hours of operation in the experimental tests mentioned above (Steele et al., 2023; Demougeot et al., 2024; Berg and Magnusson, 2023; Parsania et al., 2024). Since hydrogen will remain a scarce resource over the next decade, the GT industry defined "H_2-readiness" for new gas power plants in three levels according to the hydrogen volume content of the fuel used: 100 % hydrogen down to 25 % and 10 % hydrogen blended into NG. Moreover, three sub-categories were set to classify the technical adaptations needed to switch to the desired hydrogen level, including:

- no substantial modifications (except for the gas supply outside the plant),
- minor upgrading necessary,
- upgrading technically and economically possible

with the costs for the upgrade within 5, 10, 20 % of the overall cost of building a new power plant, respectively. The combinations of both classifications led to a common interpretation of "H_2-readiness", as shown in Fig. 1 (EUTurbines, 2021).

1.3. Hydrogen impact on gas turbine performance

With the understanding that options for hydrogen production and storage can profoundly affect the operation and even the competitiveness of hydrogen-fueled GT plants, as highlighted by Öberg et al. (2022), the focus here is on evaluating thermodynamic performance. Based on turbomachinery fundamentals, no detrimental impact on GT outputs is expected. In other words, GT power (P_{GT}) and thermal efficiency (η_{GT}) with hydrogen range from no loss to higher than with NG (Shilling and Z., 2023). However, the actual values of P_{GT} and η_{GT} are a function of the GT configuration and control used, with modeling and simulations as the main sources of information. Assuming the same turbine inlet temperature (TIT) of the exhaust gases as in the NG case, an increase in η_{GT} was found by recent studies (Skabelund et al., 2023; Mustafa et al., 2024; Morales et al., 2024; Kapoor et al., 2024), in agreement with pioneering research (Moliere et al., 2004). Bexten al. (2021) also found that η_{GT} increases progressively with the hydrogen share in the fuel, at constant TIT, although their work was more focused on exhaust gas recirculation. The same conclusion was reached with the assumption of keeping the power produced by the GT unchanged (Koç et al., 2020; Álvarez et al., 2024). Obviously, the gain in η_{GT} rises with the hydrogen share. Amrouche et al. (2025) confirmed the positive impact of hydrogen on both P_{GT} and η_{GT} under seasonal climate variations for a specific location in Southern Algeria.

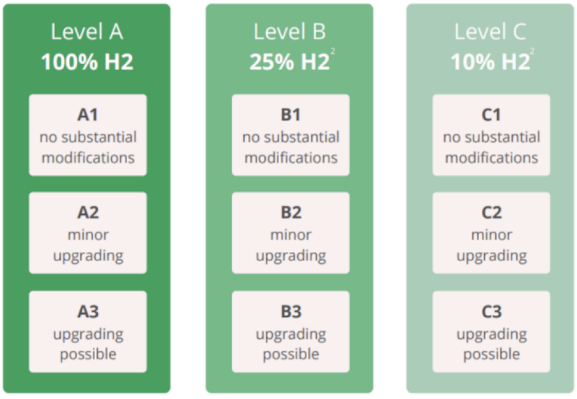

Fig. 1. H2-readiness of GT based power plants (EUTurbines, 2021).

Jeong et al. (2024) expanded the analysis to include both the SC and CC modes, under the assumption of maintaining TIT or power at a constant level. Regardless of the GT mode, the system efficiency was enhanced in both cases, with the former proving to be more advantageous, despite resulting in higher NO_x emissions. Additionally, they compared different GT models with various TIT values, determining that the benefit of hydrogen co-firing is most significant at the highest TIT. Mustafa et al. (2024) also added the CC mode to their investigation: they pointed out that an improvement in CC thermal efficiency (η_{CC}) is still obtained with increasing hydrogen content at constant turbine outlet temperature (TOT), although lower than that of the SC. Morales et al. (2024) conceived combined heat and power configurations for a CC with a simple, one-level pressure heat recovery steam generator (HRSG), without reheat. Whatever the purpose (production of electricity, steam for the user, or a combination of both), the electrical efficiency of all systems increases with the hydrogen fraction. Again, there is consistency with an earlier milestone study by Seydel (2015), in which the same TOT of NG was set. He clearly stated that hydrogen-enriched fuel makes η_{CC} increase and the performance enhancing effect is valid for the entire GT load range, although to a lesser extent at lower loads. Munther et al. (2025) adopted a different perspective: they estimated the amount of hydrogen required by a real CC power plant in Iraq over a year, with green hydrogen fractions up to 50 %, with the goal of sizing the renewable upstream chain.

1.4. Novelty and goals

However, none of the cited studies focused on dispatching strategies for gas turbines with hydrogen in the fuel stream. Providing exactly the right amount of electricity required by grid, whatever the ambient conditions, may not be sufficient when consuming high-cost fuels such as hydrogen: maintaining high efficiency is of paramount importance, despite partial load and weather conditions that may be unfavorable. For this reason, the core of the study relates to the impact of GT control strategy on η under fuel flexibility and load adjustment, given the external ambient conditions.

Two scenarios were considered driven by the ongoing energy transition. On the one hand, a SC GT peaker can start up and reach full load as quickly as possible though it is less efficient than engines used for baseload power; it operates during periods of high demand and then shuts down, running <1500 h per year, and even for as few as 250 h per year. On the other hand, a load following CC power plant operates at a lower load, hence reduced efficiency, for longer hours to offset the variability of renewables. More variables are involved than for peakers: for instance, the power output comes from combining the topping Joule-Brayton cycle with the bottoming Rankine cycle, thus highlighting the importance of the GT exhaust heat recovery to improve the sustainability of the power plant. In both cases, simulation predictions under real-world conditions can demonstrate the effects of decarbonisation through efficiency, with gas turbines bridging the gap between the past and the future of the energy landscape. Moreover, the investigated framework allowed for a fair comparison between the two fuels, NG versus hydrogen, under the same constraints in terms of external ambient conditions and required power output. Indeed, the assumption of derated GT efficiency when NG is replaced by hydrogen is quite common (ETN, 2022; Neville, 2023), but it might not be mandatory, especially in view of the recent improvements in sequential, multi-stage

combustion.

2. Modeling of GT power plants: context and assumptions

The system boundary includes the GT power plant in both modes, from fuel input to the combustor to the return of exhaust gases to the environment. Fuel production, delivery, and storage were not included in the model. All results refer exclusively to the GT in SC or CC, assuming that the fuel, whatever it may be, is ready for use. Simulations of the power plants were carried out under steady state conditions using Thermoflex® software (version 31) by Thermoflow Inc. The iterative solving of mass and energy balances, based on standard parameters such as pressure, temperature, enthalpy, and mass flow rate, was combined with user-defined control loop routines (see Appendix A1 for more details on numerical settings). In essence, control loop instructions directed the code to adjust specific control variables to achieve a targeted output value within a defined tolerance range. This approach proved effective in managing the GT behavior at part-load while meeting electricity demand.

With NG as fuel, the reliability of thermodynamic predictions was verified against GT datasheet at design point. At off-design, the numerical convergence of the simulations ensured consistency with the operating maps delivered by the manufacturers within the software platform. On the contrary, hydrogen usage required a specific validation process against the published literature (Appendix A2).

Each of the following subsections was structured to provide dual content, specifically for GT in SC and CC, respectively.

2.1. Operating environment

Hourly electrical load profiles came from the EIA database (EIA, 2023) while ambient temperature (T_{amb}) trends were obtained from the "Weather Spark" climate report (Weather Spark, 2023). They refer to the US cities of Springfield (Illinois) and New York (New York) for SC and CC, respectively. The real-world set of numbers was then scaled down to fit the format of the GT plants conceived in this study. The resulting curves are depicted in Fig. 2 on a summer and winter day. Please note that the days selected were chosen to take into account the impact of hot/cold ambient temperatures on GT performance, as extreme conditions that may occur over the course of a year.

The GT in SC mode is operational for a few hours per day. In summer (Fig. 2a), it operates from 1:00 pm. to midnight to compensate for renewables and cover the high electricity demand caused by air conditioning. In winter (Fig. 2b), it is used to meet the peak evening demand from 4:00 pm. to midnight, when industrial and residential electricity requirements add up and reach their maximum at 10 pm., subsequently declining slightly as the night progresses. Winter day is characterized by cold weather, with T_{amb} ranging from about −7 to 1 °C whereas summer brings moderate heat, with T_{amb} between 19.5 and 25.6 °C.

The CC scheduling extends over the entire day. High load variability is evident during the summer day (Fig. 2c): the typical ramp from minimum load to the late evening maximum is caused by the decline in renewable energy contribution, after the sunset. In the winter day (Fig. 2d), the peak is reduced, thereby minimizing the demand fluctuation. The ambient temperature remains below zero for most of the winter day ($-8\ °C < T_{amb} < 3\ °C$), while in summer it remains moderately warm, with the highest value being around 26 °C.

2.2. Design characterization

All ratings are based on ISO conditions and NG fuel. The ideal composition of 100 % CH_4 was assumed, with a lower heating value (LHV) of 50,047 kJ/kg.

For SC mode, GE 6B03 was selected due to its reliability and fuel flexibility, with the manufacturer declaring 55 million operating hours and a rated performance of 45 MW output and 33.4 % net efficiency. Standard combustion is capable of up to 100 % H_2 while DLN combustion supports up to 30 % H_2 (GE, 2021). The fuel stream, whatever the

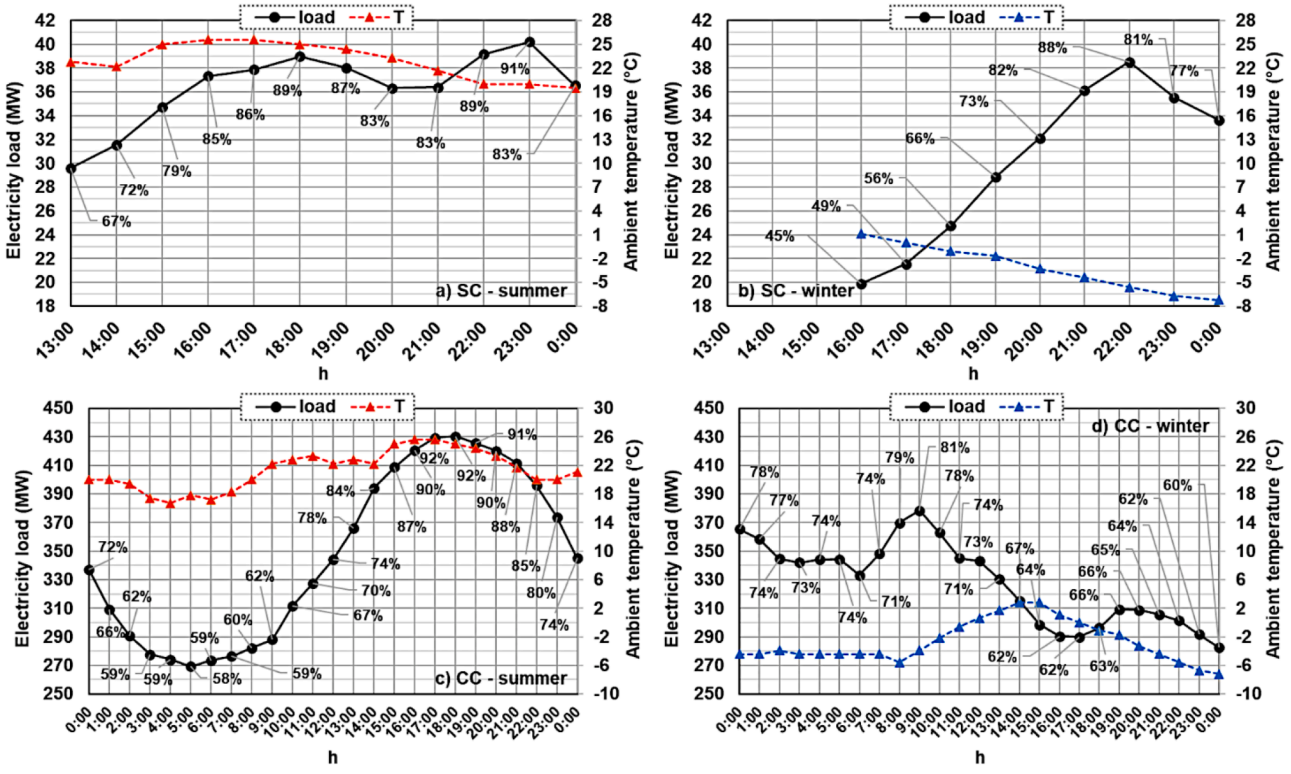

Fig. 2. Electricity load patterns and ambient temperature profiles in summer (left) and winter (right): SC (top) and CC (bottom). Data labels show the percentage ratio of the load to ISO rated net power.

composition, was assumed at a pressure enough to enter the combustor (20 bar) and 25 °C. Design features are depicted in the engine graphic of Fig. 3.

In CC arrangement, SGT5–4000F was chosen because of its potential at part-load, thanks to variable inlet guide vanes plus two stages of fast-acting variable-pitch guide vanes. The production of 329 MW is accomplished with an efficiency level of 41 %. It also tolerates fuels within a Wobbe range of ±15 %, including contents of H_2 of up to 30 vol %. For larger shares, adjustments to the DLN burner configuration may be necessary (Siemens Energy).

The output from design simulation of both GT models in SC was collected in Table 2.

Performance of the SGT5–4000F in 1 × 1 CC mode was reported in Table 3. The exhaust gas exiting the GT at approximately 600 °C enters a 3-pressure level HRSG with reheat, prior to being directed to the stack at a temperature just below 80 °C. The total number of heat exchangers in the HRSG is 12, divided as follows: four economizers, one of which is in parallel; three evaporators and five superheaters (Fig. 4a). Economizer subcooling is set between 5 and 10 °C, while evaporator pinch varies from 10 to 20 °C. The steam turbine (ST) assembly includes two high pressure (HP) stages, three middle pressure (MP) stages, and a pair of two low pressure (LP) stages operated in parallel (Fig. 4b). Steam cycle HP conditions are 150 bar/538 °C; MP admission is set at 35 bar/510 °C, after steam reheating; LP turbine admits steam at 4 bar/280 °C. Each turbine section has sliding inlet control, with dry step efficiency of 84.5, 86.2 and 90.7 %, respectively. A water-cooled condenser operating at 0.045 bar, several feedwater pumps and one deaerator (4 bar) complete the bottoming cycle. Note also that an MP feedwater line provides the thermal energy to raise the fuel temperature up to 187 °C in a preheater. The fuel pressure is assumed to be high enough to enter the combustor (31 bar). The overall CC performance is estimated at nearly 480 MW and 60 % efficiency.

The consistency with the vendor's information on generated power and efficiency is ensured within 1.5 % accuracy in all three cases (GE 6B03 - SC; SGT5–4000F - SC; SGT5–4000F - CC).

Table 2
GT design data (ISO conditions; fuel: NG).

Parameters	GT - SC	
GT Model	GE 6B03	SGT5–4000F
Gross/Net power (MW)	44.65/43.96	329.7/325.1
Net efficiency - LHV (%)	33.54	40.48
Inlet air (kg/s)	141.9	701.6
Compressor pressure ratio	12.71	19.01
Fuel flow rate (kg/s)	2.619	16.05
Fuel LHV (kJ/kg)	50,047	
Turbine inlet temperature (°C)	1149.9	1372
Exhaust mass flow (kg/s)	144.5	717.7
Exhaust temperature (°C)	550	603.2

Table 3
CC design data (ISO conditions; fuel: NG).

Parameters	Value
CC Gross/Net power (MW)	480.8/467.4
CC gross/net efficiency - LHV (%)	60.14/58.46
GT model	SGT5–4000F
ST power (MW)	160.8
Superheater/Economiser water-side pressure drop	2 %
Evaporator Blowdown	1 %
Superheater/Evaporator/Economiser heat loss	0.75 %
Stack temperature (°C)	77.5

2.3. Off-design characterization with conventional fuel

For a GT in SC, it is widely recognized that the most effective part-load control implies lowering the fuel flow (m_f) at constant air inlet (m_a), according to the so-called TIT/fuel control (Elmasri, 2009). Consequently, TIT decreases in conjunction with TOT. This also reduces the compressor pressure ratio (β) with the turbine behaving as a choked nozzle. The penalty in η_{GT} is less significant than that resulting from alternative strategies based on lowering the intake air for a given load. Fig. 5 shows GE 6B03 behavior under TIT/fuel control: the linear decrease of fuel flow (Fig. 5a) is responsible for the reduction in TIT and TOT (Fig. 5b), which corresponds to a progressive decay of η_{GT} as the load is reduced. At a minimum load of 20 % η_{GT} drops to 18.24 %; at half load the loss in η_{GT} is about 5 pp compared to the design point.

For a GT in CC, heat recovery from exhaust gases aimed at producing additional power through bottoming Rankine cycle attaches importance to TOT. That is why load reduction is typically accomplished by lowering m_a through the IGV closure. If TIT is kept almost constant at the nominal value, TOT rises. As a result, a smaller amount of hotter flue gas is sent to the HRSG, thus improving heat recovery by lowering stack temperature. Indeed, a combination of fuel (TIT control) and air modulation (IGV control) can be exploited to achieve the target value of TOT, set to boost η_{CC} while preserving the life of the last uncooled turbine stages. In light of this, this work adopted a user-defined (UD) partial load control based on the "XIGV" parameter available in the modeling

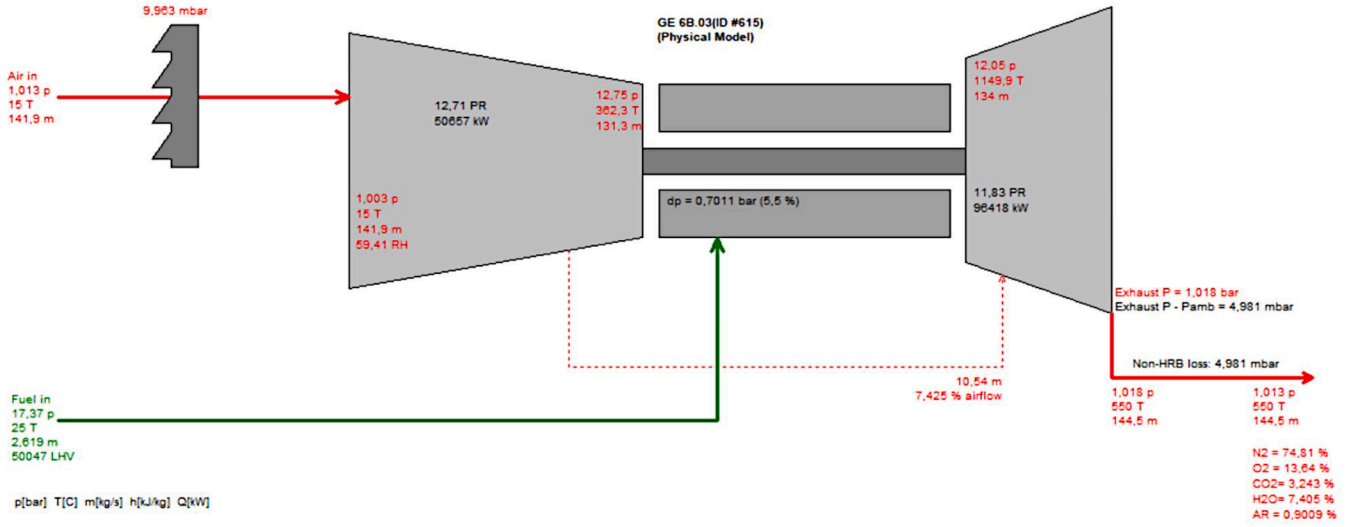

Fig. 3. Design point of the GE 6B03 in SC mode (screenshot of Thermoflex®).

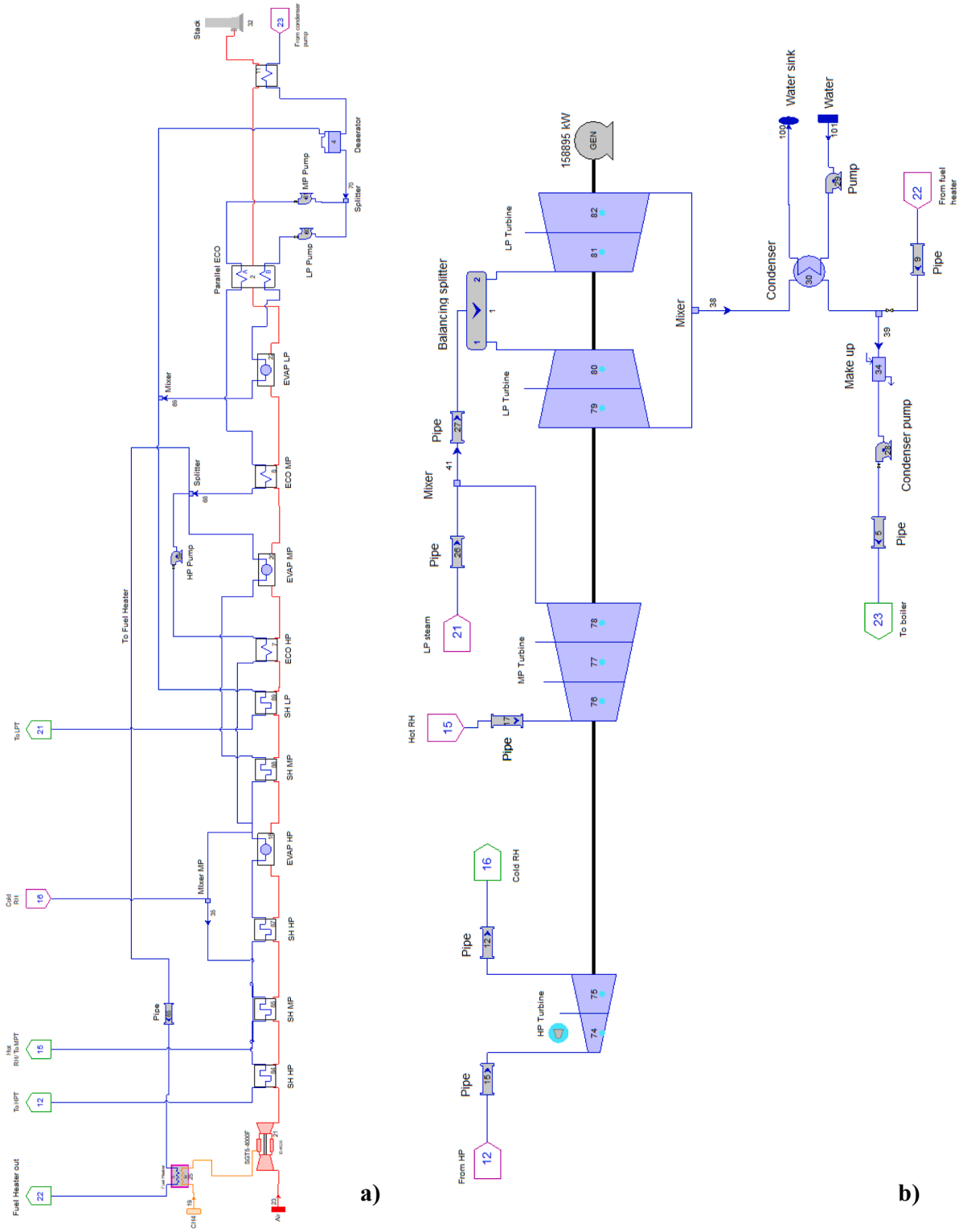

Fig. 4. CC layout: a) GT and HRSG; b) steam turbine and water-cooled condenser (screenshot of Thermoflex®).

code. Please note that XIGV can vary from 0 to 10, with each value corresponding to a specific combination of m_a, fuel flow, TIT and TOT. Through an iterative search within 0 < XIGV< 10, the desired trend of TOT was obtained (Fig. 6). For the SGT5–4000F in CC mode, the UD TOT was allowed to increase as the load decreases, within the maximum limit of 50 °C above the nominal value (Elmasri, 2009). The peak TOT of 645 °C complies with this constraint and occurs at a GT load of 65 %; a decreasing trend is established at lower loads. Conversely, the pre-programmed scenario implemented in the code (labeled as "pre") involved keeping TOT constant at the design value over the widest possible load range. For GT load ≤ 30 %, both solutions coincide: as the minimum airflow is reached (424.8 kg/s) the constant TOT is necessarily abandoned as firing temperature continues to fall to further reduce load to the minimum turndown. The corresponding TIT profiles are also shown in Fig. 6: slightly higher values within 30 %<GT load<100 % characterize the UD case with the maximum increase over the

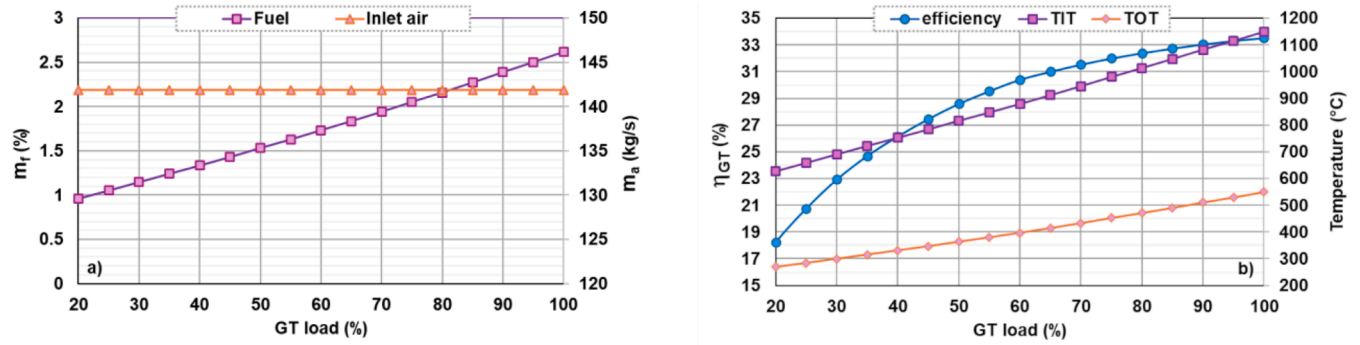

Fig. 5. GE 6B03 part-load performance (ISO conditions, fuel: NG): a) fuel and inlet air flow; b) TIT, TOT and efficiency.

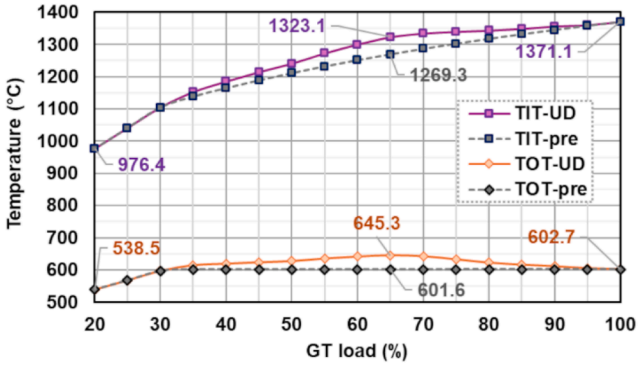

Fig. 6. SGT5–4000F_CC mode part-load performance in pre-programmed (pre) and user-defined (UD) scenario: TIT and TOT (ISO conditions, fuel: NG).

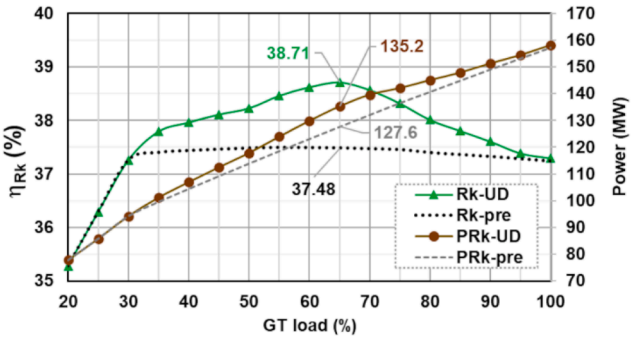

Fig. 8. SGT5–4000F_CC mode part-load performance in pre-programmed (pre) and user-defined (UD) scenario: efficiency and power of the bottoming Rankine cycle (ISO conditions, fuel: NG).

alternative option of 54 °C at 65 % GT load. This is the price to pay for higher $\eta_{CC,n}$ at part-load (Fig. 7), with the largest increment of 0.7 pp: the explanation is that the enhancement in Rankine cycle efficiency (η_{Rk}), reaching up to 1.2 pp (refer to Fig. 8), surpasses the reduction in $\eta_{GT,}$ which is confined within 0.5 pp. Moreover, the power delivered by the bottoming cycle increases up to 7.7 MW. It is worth mentioning that η_{Rk} is greater than or equal to η_{GT} within GT load $\leq$ 80 % when applying UD control. Therefore, a shift in power production from the topping to the bottoming cycle may be advantageous. In the best case, the loss in $\eta_{CC,n}$ is 4.7 pp at half load and grows to about 10 pp at 30 % GT load (Fig. 7).

To complete the off-design characterization of GE 6B03 and SGT5–4000F, correction factors were computed for P_{GT} and η_{GT} as a function of T_{amb}, at full load (Fig. 9). Both GTs are negatively affected by

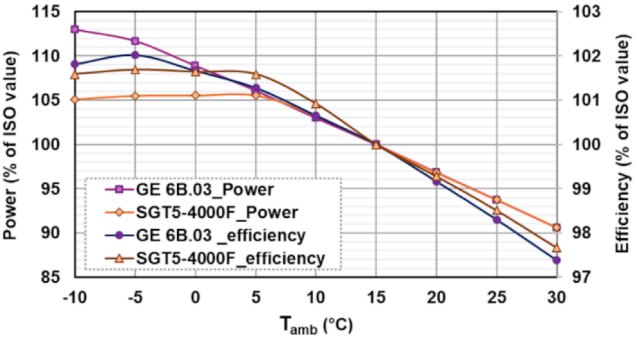

Fig. 9. GT correction curves as a function of inlet temperature (full load, fuel: NG).

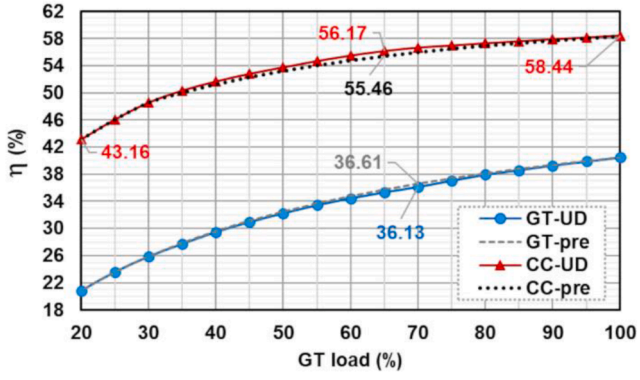

Fig. 7. SGT5–4000F_CC mode part-load performance in pre-programmed (pre) and user-defined (UD) scenario: GT and CC efficiency (ISO conditions, fuel: NG).

warm weather, to a similar extent: at T_{amb} of 30 °C, P_{GT} decreases roughly by 10 % with a loss in η_{GT} of 2.6 and 2.3 pp, respectively, compared to ISO conditions. Conversely, their behavior differs at T_{amb} lower than 15 °C. For GE 6B03, P_{GT} can exceed the nominal value by up to 13 %, with a 2 % gain in η_{GT} in cold weather ($T_{amb} = -10$ °C). In contrast, the maximum output of SGT5–4000F is limited by the capacity of the generator when $T_{amb} \leq 5$ °C. The largest P_{GT} remains within 106 % of the design rate, corresponding to a 1.7 % increase in η_{GT}.

It should be clarified that all GT performance data displayed in this section were obtained from technical information supplied by manufacturers and integrated into the simulation software. Sources are GE GTP Web 4.23.0 for GE 6B03 and Siemens SIPEP 5.14.0 for SGT5–4000F. Even the UD strategies are consistent with the real GT operating maps under the constraint that simulation convergence is achieved. Therefore, no further validation of the model predictions is needed when the fuel fed to the GT is NG.

3. Results and discussion

The power plant models were instructed to deliver a power output equal to the electricity load of Fig. 2, within the tolerance of 0.001 %, by adjusting the GT load. This was accomplished through a "master" control loop configured in Thermoflex® in both SC and CC scenarios (see Table 4). In detail, the electricity load was imposed equal to the gross power (P_g) at the generator terminals for SC case and to the total net power (P_n) in CC case. An additional "secondary" loop was necessary to manage the UD control strategy of the SGT5–4000F in CC mode. As outlined in Section 2.3, XIGV is the control variable to be changed to achieve the TOT as specified by the user. Obviously, the site T_{amb} was also imposed to align with the dashed profiles depicted in Fig. 2. The time step was one hour, i.e., large enough to neglect transient dynamics.

Given the consensus of published literature on the beneficial effects of hydrogen use on the GT thermodynamic performance, a comparison was made between pure H_2 and NG as fuel: the objective was to ascertain the maximum gain achievable from the decarbonized fuel in a realistic context.

3.1. Peaker GT in SC

This section contains the simulation outputs related to GE 6B03 operated in SC under the load constraints of Figs. 2a and 2b, during both summer and winter days. The discussion on Joule-Brayton cycle parameters facilitates a performance assessment in terms of η_{GT} under the influence of fuel flexibility.

3.1.1. Thermodynamics of the Joule-Brayton cycle

Consistent with the part-load control illustrated in Section 2.3, m_a does not vary with GT load; it is solely influenced by T_{amb}, due to the effects on air density at the compressor inlet (Fig. 10a). Whatever the fuel, the lower the T_{amb}, the greater the airflow: on winter day, cold weather allows high levels of m_a exceeding 150 kg/s while warm weather drops m_a to a minimum of about 136 kg/s when T_{amb} remains around 25 °C (from h. 15 to 18 in summer). For all other variables involved in GT regulation, load has a dominant impact, so their profiles follow electricity demand. This is all the more valid for the fuel supply (Fig. 10b): m_f is proportional to the desired power output, given the available m_a. Much more interesting is the effect of fuel quality. As the LHV increases to 120 MJ/kg from 50 MJ/kg when NG is replaced by H_2, there is a corresponding reduction in fuel requirements. A hydrogen flow rate between 0.6 and 1 kg/s is sufficient to meet the GT needs for both days, compared with a NG range of 1.4 to 2.4 kg/s.

Therefore, for a given m_a, hydrogen combustion produces fewer exhaust gases for subsequent expansion in the turbine. Furthermore, their chemical composition undergoes a change (Table 5): the expected reduction of CO_2 content, which is below 0.03 % vol on both days, is somewhat offset by an increase in H_2O mole fraction, up to 11.5 %. Also, there is a slight increase in oxygen percentage. Hence, gas thermodynamic properties vary as well: in particular, specific heat at constant pressure (c_p) and volume (c_v), as well as gas constant (R) and specific heat ratio (γ) grow with H_2O fraction. All this contributes to a redefinition of the compressor-turbine matching, as the author (Ravelli, 2022) previously noted, following the path laid out by the landmark study by Chiesa et al. (2005). Although performance maps of the compressor and turbine are not publicly available from the manufacturer, it has been verified that the predicted running point with hydrogen correctly restores the equilibrium between the two turbomachines that was originally conceived for NG. In fact, the turbine operates under the chocked condition expressed by:

$$\frac{m_i\sqrt{R\,T_i}}{p_i} \sim Constan \tag{1}$$

The decrease in turbine inlet flow (m_i), due to the lower m_f, is accompanied by a reduction in turbine inlet pressure p_i, thus β, and in turbine inlet temperature (T_i = TIT), so that the result of Eq. (1) is constant, despite the increase in R. Fig. 11 quantifies the extent of the reduction for both parameters, β and TIT, maintaining the dynamics imposed by the electrical load. The largest drop in β is 0.50 % and 0.39 % in summer (at h. 17) and winter (at h. 21), respectively (Fig. 11a). The corresponding decrease in TIT is 1.78 % and 1.59 % (Fig. 11b). For completeness, Fig. 12 demonstrates the effect of the flue gas composition on R: higher values with hydrogen as fuel depend on the larger H_2O mole fraction at the expense of CO_2. The four main variables in Eq. (1) results in a constant corrected flow at turbine inlet of 0.0717 ± 0.0001, regardless of the load, T_{amb} and fuel type. Also, flue gas expansion ends at lower temperatures: the largest reduction in TOT is 2.25 % in summer and 2.02 % in winter (Fig. 13), with all TOT profiles mimicking the load.

Despite the lower TIT and β, the use of hydrogen ensures the highest η_{GT} (Fig. 14a), with a gain (see labels) that increases in proportion to the electrical demand. This is due to the fact that the total heat input to the combustor is lower for the same power output, in agreement with the dissertation provided by Jeong et al. (2024), with specific reference to "Case 3 - gas turbine with fixed power". Values of $\Delta\eta_{GT}$ range from 0.46 up to 0.59 during the summer day while in winter $\Delta\eta_{GT}$ varies between 0.31 and 0.49, peaking at the hour of maximum demand. The GT best performance is characterized by η_{GT} of 33.6 % across both days. Conversely, the smallest value of η_{GT} is dependent on the selected day: it drops to 27.8 % in winter at the lowest grid demand while it remains above 31.5 % in summer. This is in alignment with GT load: it is relatively high, i.e., above 75 %, in summer whereas more severe part-load conditions are experienced in winter, when values between 40 and 75 % were computed. In addition, it is noteworthy that the GT load with hydrogen as fuel is always lower than with NG (Fig. 14b), because of the augmented GT rated capacity (46.44 vs. 44.65 MW): their difference, as indicated in the labels, ranges from 1.7 to 4.0 pp.

3.1.2. Influence of hydrogen on GT performance

To further explore the effects of hydrogen on GT performance, the increase in η_{GT} due to the replacement of NG with H_2 was charted as a function of electricity load (Fig. 15a). It is easy to deduce that the level of benefit grows with the power demand. Furthermore, it appears that summer conditions are associated with higher values of $\Delta\eta_{GT}$ than winter ones. This is attributable to the higher GT load necessary to meet the prescribed power output when the compressor intake air is reduced by warm weather. In fact, Fig. 15b clearly shows that the leading parameter is the GT load, which exhibits a positive, linear relationship with $\Delta\eta_{GT}$. This latter decreases from 0.6 to 0.3 pp when the GT load is reduced from 90 % to 40 %.

3.2. Load following GT in CC

In this section the discussion focuses on the simulation outputs related to SGT5–4000F operated in CC under the load constraints of Figs. 2c and 2d, considering both summer and winter days. The reader is reminded that the UD part-load control was applied because of its superior performance, in terms of $\eta_{CC,n}$, compared with the pre-programmed strategy, as demonstrated in Section 2.3. The main CC thermodynamic parameters are reviewed to determine the influence of fuel on η_{CC}.

Table 4
Simulation controls.

Controls	Master loop (I)	Master loop (I)	Secondary loop (II)
Applicability	SC	CC	CC
Target	P_g = Load	P_n = Load	TOT = UD TOT
Control variable	GT load	GT load	XIGV
Range	20 % - 100 %	20 % - 100 %	0–10
Tolerance	0.001 %	0.001 %	3 °C

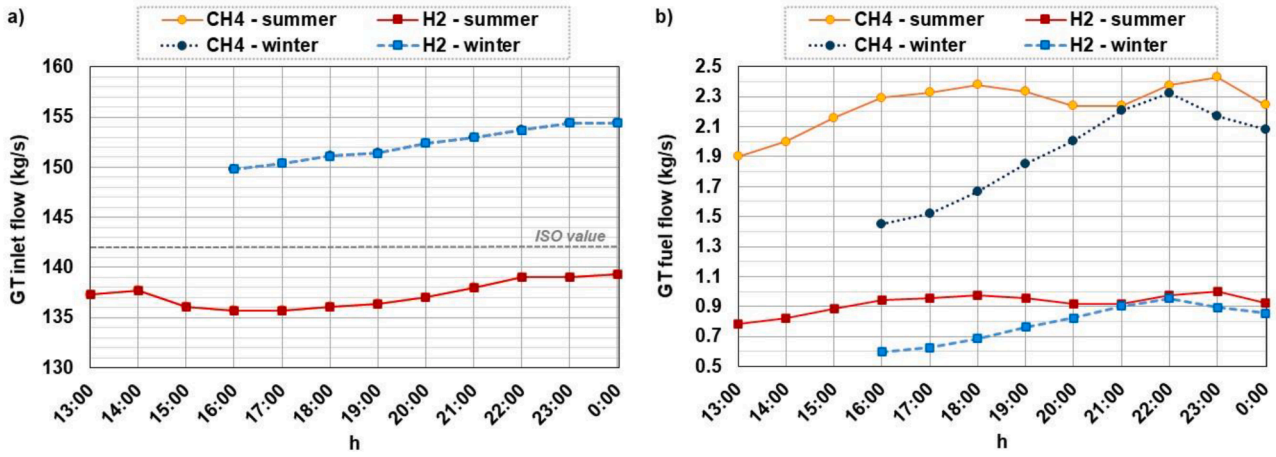

Fig. 10. GT inlet airflow (a) and fuel flow (b) in summer and winter day: NG vs. H_2.

Table 5
Flue gas at turbine inlet: composition and properties (GE 6B03).

	Winter day			Summer day		
mol %	**CO_2**	**H_2O**	**O_2**	**CO_2**	**H_2O**	**O_2**
CH_4	1.7–2.7	3.8–5.5	15.0–17.1	2.6–3.1	6.6–7.9	13.9–15.0
H_2	<0.029	5.9–8.7	15.8–17.5	<0.029	9.4–11.5	14.7–15.9
(J/kg-K)	**R**	**c_v**	**c_p**	**R**	**c_v**	**c_p**
CH_4	289.6–290.7	0.861–0.926	1.151–1.216	291.9–292.9	0.926–0.976	1.218–1.269
H_2	294.5–298.2	0.872–0.943	1.166–1.242	298.8–301.6	0.943–0.997	1.241–1.299

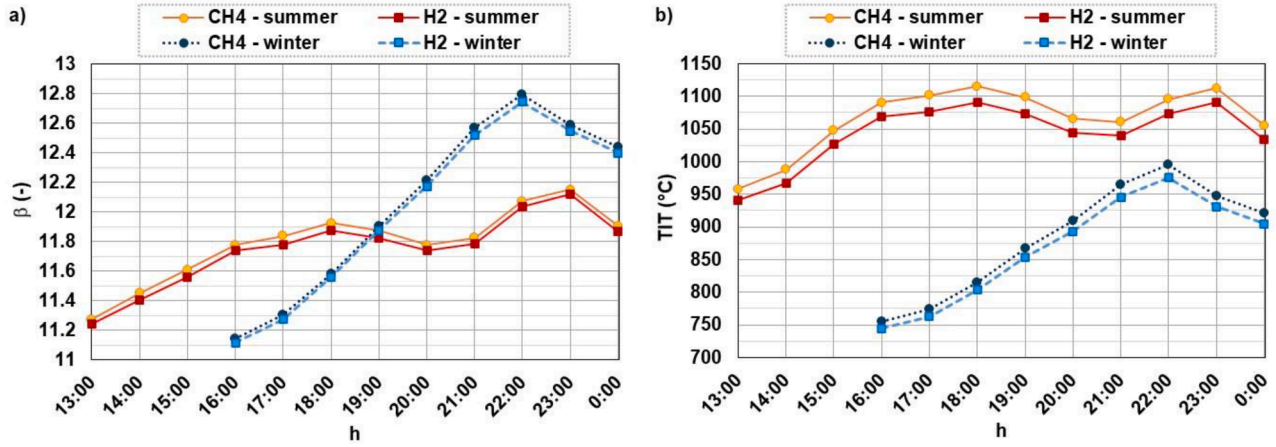

Fig. 11. GT compressor pressure ratio (a) and TIT (b) in summer and winter day: NG vs. H_2.

3.2.1. Thermodynamics of the CC

The combination of both master and secondary control loops was effective in finding the values of m_a (Fig. 16a) and m_f (Fig. 16b) that reflect the daily pattern of electricity load, while allowing TOT to rise above the design value within the maximum threshold of 645 °C (Fig. 16c). Indeed, profiles of TOT show variations within a very narrow range, i.e., around 10 °C, which depend mainly on the load and convergence tolerance of the numerical method rather than the fuel type. This is also the case for TIT, which is governed predominantly by the electricity load (Fig. 16d): the rule is that the higher the load the higher the TIT. Therefore, values well below the design point, within 1253 °C<TIT< 1342 °C, were computed for the entire winter day, due to the combination of low loads and cold climate. But even in summer day, when high loads occur in conjunction with warm weather, from h. 16 to 20, the increase over the rated value is limited to about 10 °C (1370 °C < TIT < 1381 °C), thus confirming the applicability of the proposed method in view of the need to maintain the durability of the hot gas-path components. The fuel used does not affect TOT and TIT, but m_a and m_f: both are lower in the case with H_2 to take into account the higher LHV, within the constraint imposed by the constant corrected mass flow though the turbine (equal to 0.2524 ± 0.0004). The extent of the reduction in m_a is within 4 % on both days, while that of m_f is in the order of 59 %. The resulting reduction of m_i is within 5.4 %, consistently with a decrease in β ranging between 2 and 3 % (Fig. 17a). This ensures the validity of Eq. (1) although the increase in R. In fact, regarding the chemical composition and properties of the combustion products, the considerations made in Section 3.1 remain applicable. The exhaust enters the turbine section with higher c_p, c_v and R due to the larger H_2O fraction coming from H_2 oxidation, as detailed in Table 6. This phenomenon is particularly pronounced during the summer day, when the

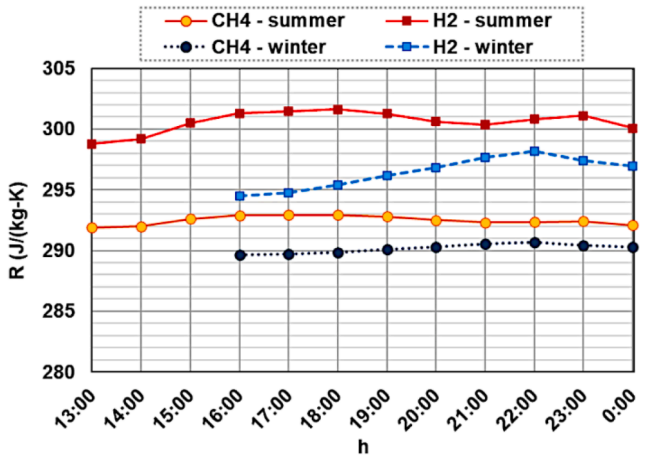

Fig. 12. Gas constant at turbine inlet in summer and winter day: NG vs. H_2.

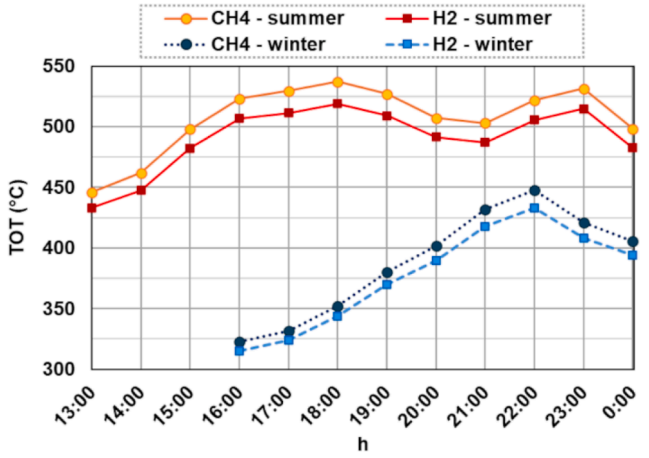

Fig. 13. GT TOT in summer and winter day: NG vs. H_2.

maximum H_2O fraction of 15 % is recorded from h. 16 to 20. Trends of β go hand in hand with the GT load (Fig. 17b): the juxtaposition of Fig. 17a and 17b reveals that, at half load, β falls to 12–13 while the high demand plateau, when GT is approaching full load, is characterized by β of 16–17. During the winter night, the GT load of about 60 % implies β of almost 14. Notwithstanding the fact that β is lower, at the same TIT, the adoption of H_2 yields higher η_{GT} attributable to the reduced external heat input required (Fig. 18a), as evidenced in Section 3.1. The gain in η_{GT} (indicated in the labels) spans from 0.60 to 0.83 pp on both days. This even more advantageous than the SC case, in agreement with Jeong et al. (2024) who suggested that the higher the TIT level, the more pronounced is the positive effect of hydrogen firing on GT performance. With H_2, the early morning dip in summer load is met with a η_{GT} of 32.9 % whereas a steep rise to the maximum value of η_{GT} = 39.7 % ensures coverage of the evening peak demand. On the winter day, the difference between the extreme values of η_{GT} is smaller, with the minimum of 33.5 % at midnight and the maximum of 37.9 % at h. 9.

Further insights were gained from the turbomachinery polytropic efficiency (n_y): for the turbine, hydrogen has a beneficial effect on n_y across the entire load range, with an increase of between 0.8 and 1 pp occurring at GT load > 20 %. In contrast, the compressor was marginally affected by the fuel change: calculations yielded a slightly lower n_y, with a small penalty of 0.12±0.02 pp at GT load > 40 %.

Although the variation in GT exhaust flow induced by GT load adjustment, η_{Rk} is quite stable suggesting that TOT is the main parameter controlling heat recovery, hence steam production in the bottoming cycle (Fig. 18b). In particular, achieving the highest possible TOT whatever the fuel, as prescribed by the UD strategy, led to high η_{Rk} values ranging from 38.2 to 38.6 %. It follows that the bottoming cycle is always more efficient than the topping one, with the exception of h. 14–23 on summer day. In this time slot, the ratio of ST shaft power (P_{ST}) to CC gross power ($P_{CC,g}$) is at the lowest level, i.e. below 37 % (Fig. 19a). The role played by ST in power generation is reinforced at low loads: it peaks at 43 % when demand drops at h.5 on the summer day and settles between 36.5 and 41.5 % on the winter day. It has to be pointed out that the fraction of $P_{CC,g}$ covered by ST is always slightly lower with H_2 as fuel, due to the reduced amount of exhaust gas entering the HRSG, at the same temperature as in the case with NG, thus lowering the total heat transfer to water/steam side by up 2 %, which is followed by a reduction in the steam flow rate available in the ST.

3.2.2. *Influence of hydrogen on CC performance*

Thanks to the virtuous logic of power distribution between GT and ST, the levels of $\eta_{CC,n}$ depicted in Fig. 19b were obtained. Once again, H_2 exerts a favorable influence on performance: the increase in $\eta_{CC,n}$, between 0.44 and 0.57 pp is comparable on both days. This range of $\Delta\eta_{CC,n}$ aligns with the findings reported by Jeong et al. (2024) in relation to "Case 4 - gas turbine combined cycle with fixed power". When NG is replaced by H_2, the swing in summer load between h. 5 and h 18 is satisfied with a $\eta_{CC,n}$ rising from 54.4 % to 59.1 %. During the winter day, the less challenging fluctuations in demand levels can be met with $\eta_{CC,n}$ varying between 54.1 % (at midnight) and 57.2 % (at h. 9).

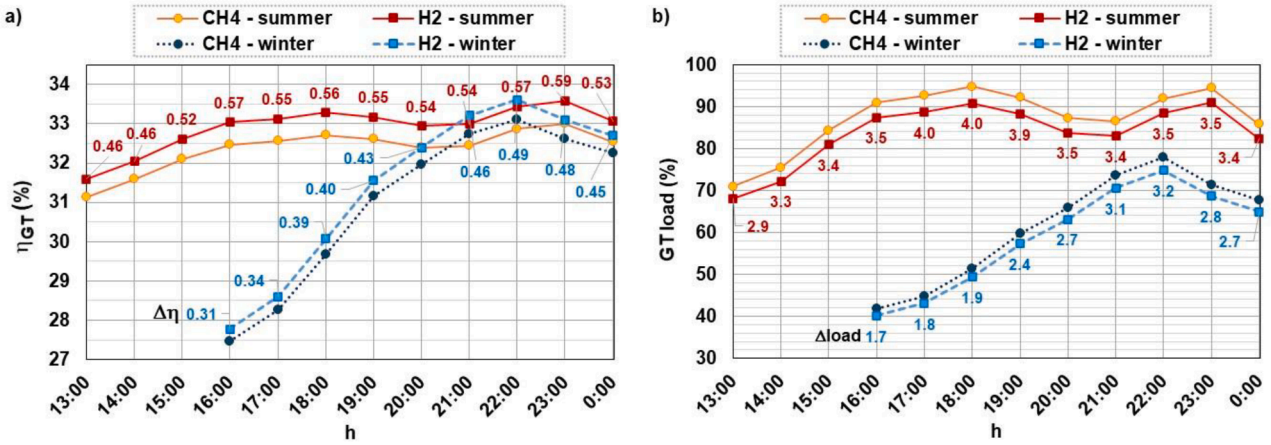

Fig. 14. GT thermal efficiency (a) and GT load (b) in summer and winter day: NG vs. H_2. Data labels show the increase in η_{GT} and the reduction of GT load due to H_2.

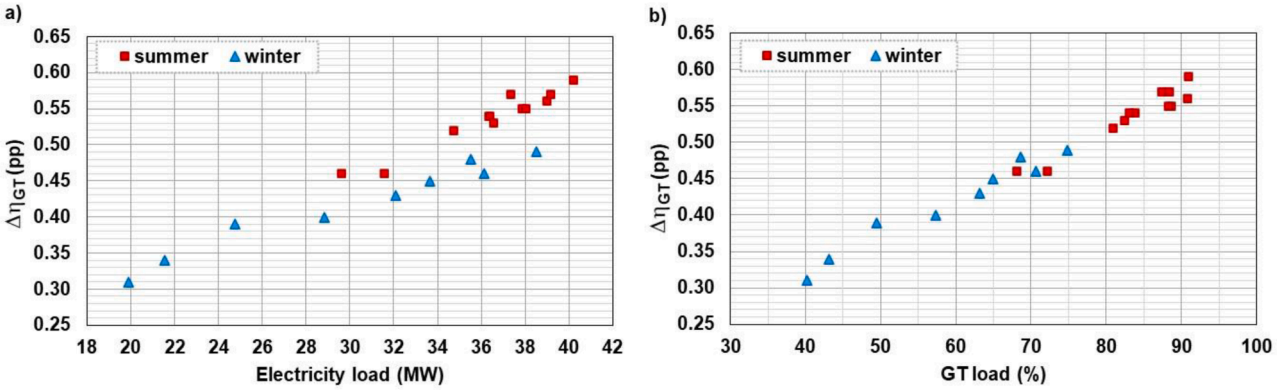

Fig. 15. $\Delta\eta_{GT}$ due to H_2, compared to NG, as a function of electricity load (a) and GT load (b).

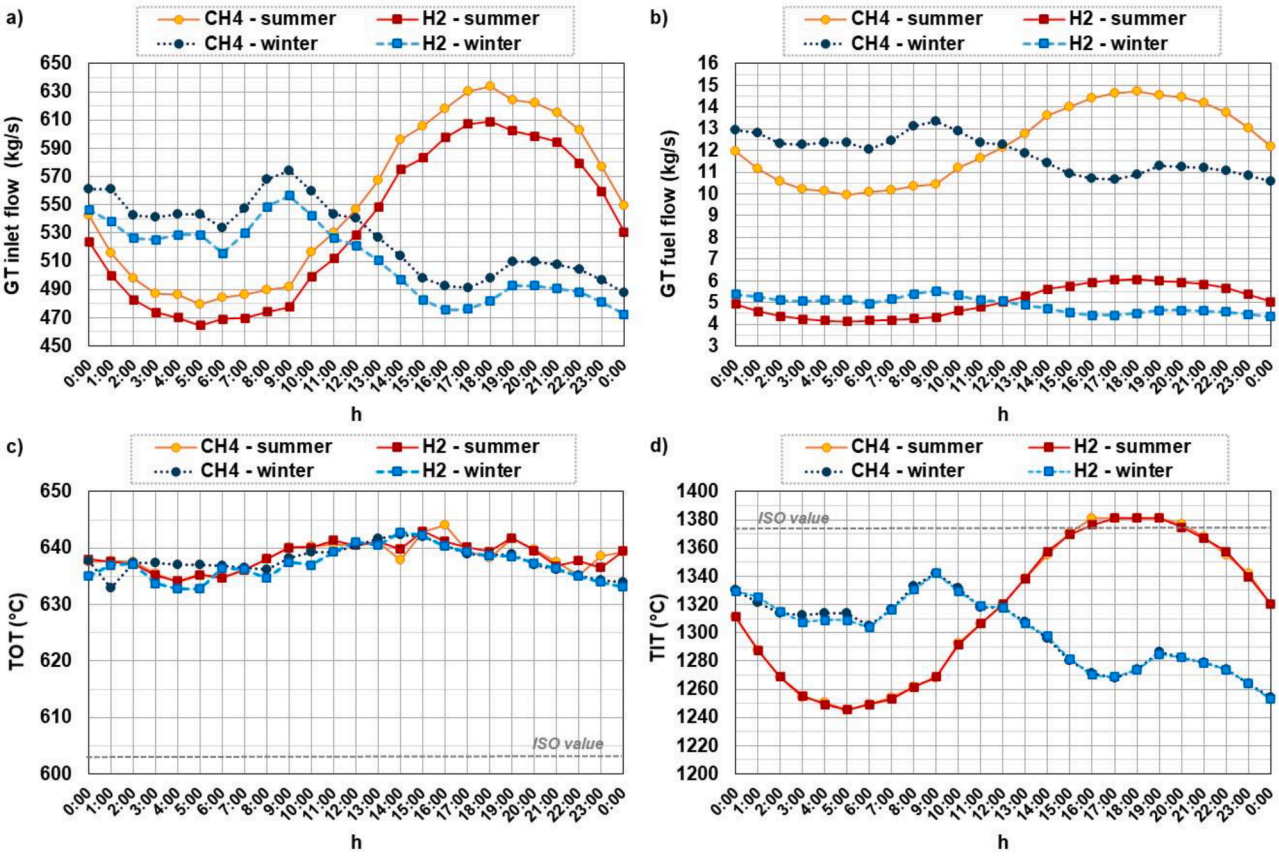

Fig. 16. GT inlet flow (a), fuel flow (b), TOT (c) and TIT (d) in summer and winter day: NG vs. H_2.

3.3. Critical assessment of combustion conditions

The combustion process was further evaluated in terms of overall equivalence ratio (Φ), defined as the actual fuel-air ratio to the stoichiometric fuel-air ratio of the reaction considered:

$$\Phi = \frac{m_f/(m_a - m_c)}{(m_f/m_a)_{st}} \quad (2)$$

The numerator of Eq. 2 takes into account the fact that about 7.5 % and 6.3 % of the intake air flow through the GT bypasses the combustor for cooling, for GE 6B03 and SGT5–4000F, respectively. Therefore, coolant extraction (m_c) reduces the actual air available at the combustor inlet. Profiles of Φ are provided in Fig. 20a and 20b for the SC and CC case, respectively. There is an almost linear dependence of Φ on GT load, regardless of GT model and mode of operation. As expected, part-load implies a lower Φ than base load. With reference to published literature, the latter is typically associated with Φ in the range of 0.45−0.6 (Jansohn, 2013) whereas Φ values from 0.15 to 0.25 are compatible with modern GT engines operated at the lowest loads (Giacomazzi, 2013). More generally, Φ levels below 0.6 are currently applied to mitigate NO_x formation and emissions. The modelling results displayed in Fig. 20 thus appear to be realistic. However, the key point is that switching from NG to H_2 leads to even leaner conditions, everything else being equal: for GE 6B03, Φ decreases from [0.18–0.33] to [0.15–0.27] whereas, for SGT5–4000F, it drops from [0.38–0.43] to [0.32–0.36]. This agrees with the conclusions drawn by Skabelund et al. (2023): they developed a GT thermodynamic model, coupled with combustion chemical kinetics, and found that the addition of H_2 in the fuel mixture

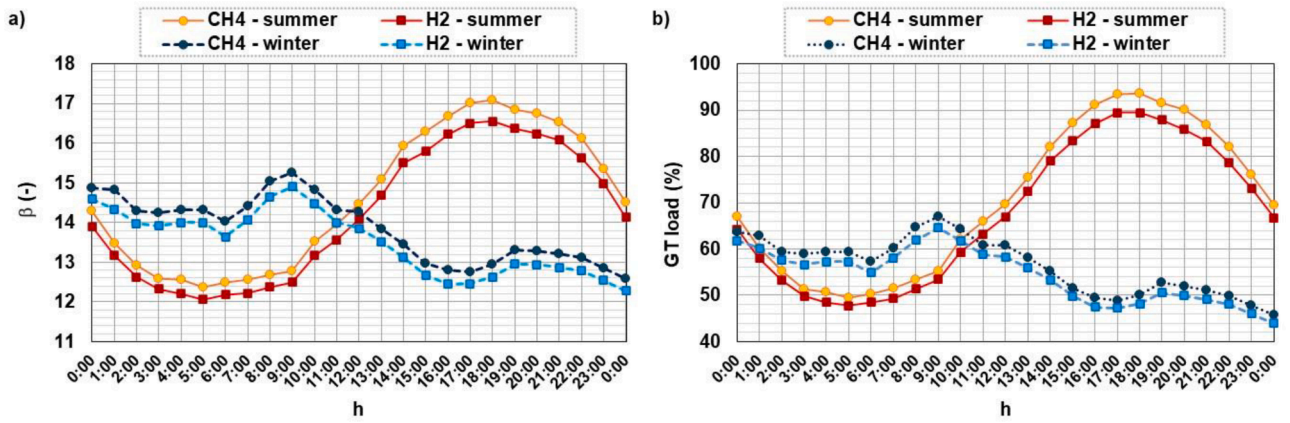

Fig. 17. GT compressor pressure ratio (a) and GT load (b) in summer and winter day: NG vs. H_2.

Table 6
Flue gas at turbine inlet: composition and properties (SGT5–4000F).

	Winter day			Summer day		
mol %	**CO_2**	**H_2O**	**O_2**	**CO_2**	**H_2O**	**O_2**
CH_4	3.8–4.06	7.7–8.3	12.0–12.6	3.6–4.04	8.3–9.9	11.7–12.8
H_2	<0.029	12.6–13.6	12.8–13.4	<0.029	13.0–15.1	12.5–13.5
(J/kg-K)	**R**	**c_v**	**c_p**	**R**	**c_v**	**c_p**
CH_4	292.1–292.5	1.006–1.033	1.298–1.326	292.9–294.3	1.011–1.060	1.304–1.355
H_2	303.4–304.7	1.046–1.079	1.350–1.384	303.8–306.5	1.050–1.107	1.354–1.414

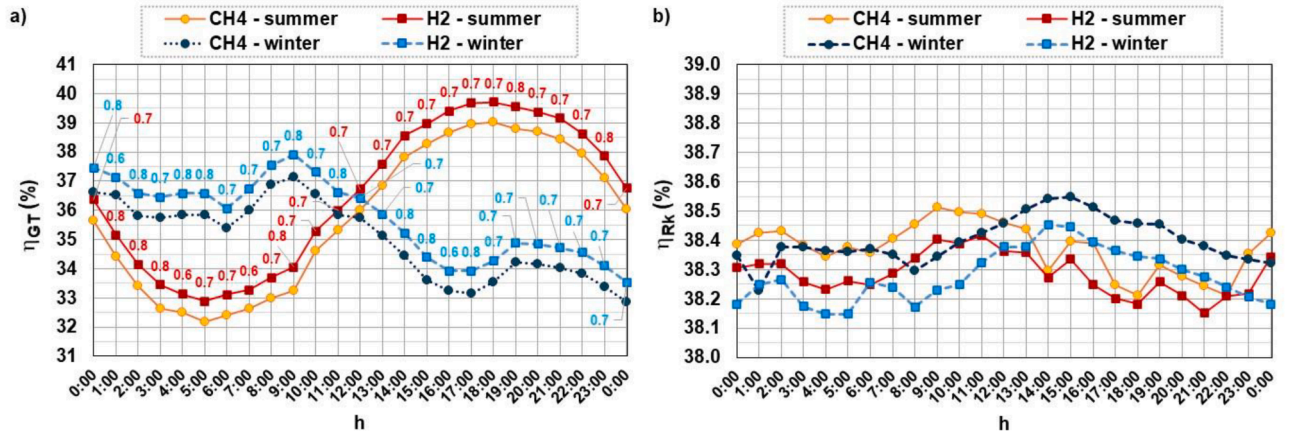

Fig. 18. GT thermal efficiency (a) and bottoming Rankine cycle efficiency (b) in summer and winter day: NG vs. H_2. Data labels show the increase in η_{GT} due to H_2.

allows operation at leaner conditions. Moreover, the lower flammability limit of the system is reduced, as is the lean blowoff limit.

As far as emissions are concerned, given the higher stoichiometric flame temperature of H_2 compared to NG, the effect of H_2 would be an increase in NO_x (Andrews, 2013). In view of this, a conservative approach was taken: values of TIT calculated with H_2 are lower (see Fig. 11b) or at most equal (see Fig. 16d) to those with hydrocarbon fuel. However, experimental campaigns are demonstrating that adjustments to air and fuel mixing by means of TOT control can keep NO_x emission within the levels of NG-only operation. This is true not only for H_2 co-firing (Berg and Magnusson, 2023; Harper et al., 2023, 2025) but also in the case of 100 % H_2 (Parsania et al., 2024; Ciani et al., 2024), provided that sequential/staging combustor tuning is carried out, i.e., the fuel split in the stages/circuits of the burner is changed. Due to the complexity of the phenomena involved in the control of auto-ignition and flame stabilization, no correlation for NO_x prediction was included in this study, pending further testing with pure H_2. According to the current level of knowledge, as hydrogen in the fuel mix increases, the flame stability enhances so pilot fractions can be reduced, thus allowing to control NO_x production. Instead, if the fuel splits are kept constant, NO_x increases with H_2 content, as expected (Parsania et al., 2024). Theoretically, in a sequential combustion which combines two staged burners, such as that of Ansaldo GT36 engine, high reactivity of hydrogen allowed for reducing fuel flow to the first stage and increasing fuel flow to the second stage, maintaining the original burner exit temperature, thus TIT, and power output (Pennell et al., 2023). Furthermore, no change in burner geometries is required to accommodate fuel flexibility, while keeping low NO_x emissions. In practice, GT36 single can test run at full pressure conditions showed that NO_x emissions were kept within project limits by reducing the normalized exit temperature, thus TIT, from 0.4 to 0.3 when the hydrogen fraction was raised above 90 % vol (Fig. 21, time 20.10 of the 4-hour test). From an abrupt estimate, this might cause a reduction in η_{GT} by about 1 pp. Nevertheless, as stated by Ciani et al. (2024), reaching 100 % hydrogen

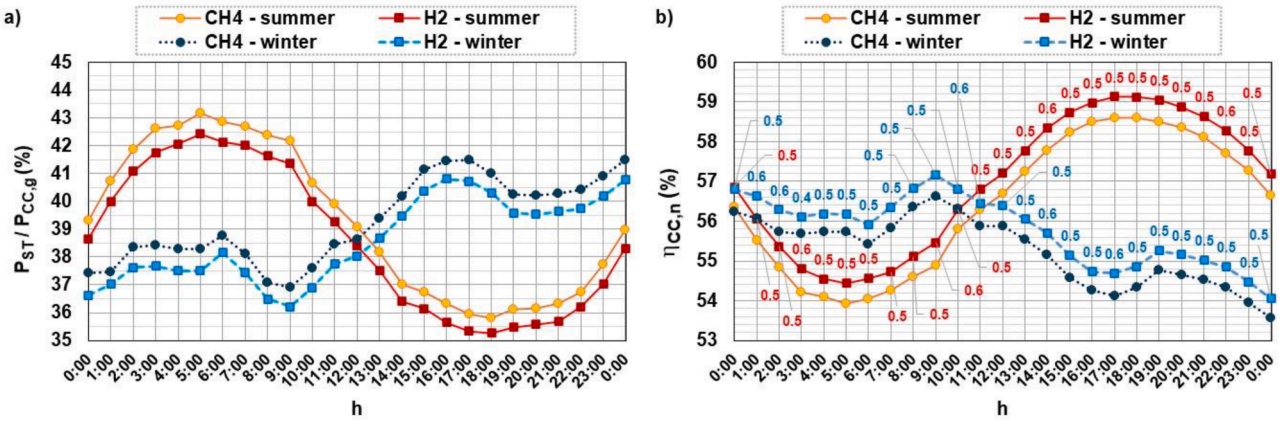

Fig. 19. Ratio of ST gross power to CC gross power (a) and CC net thermal efficiency (b) in summer and winter day: NG vs. H_2. Data labels show the increase in η_{CC} due to H_2.

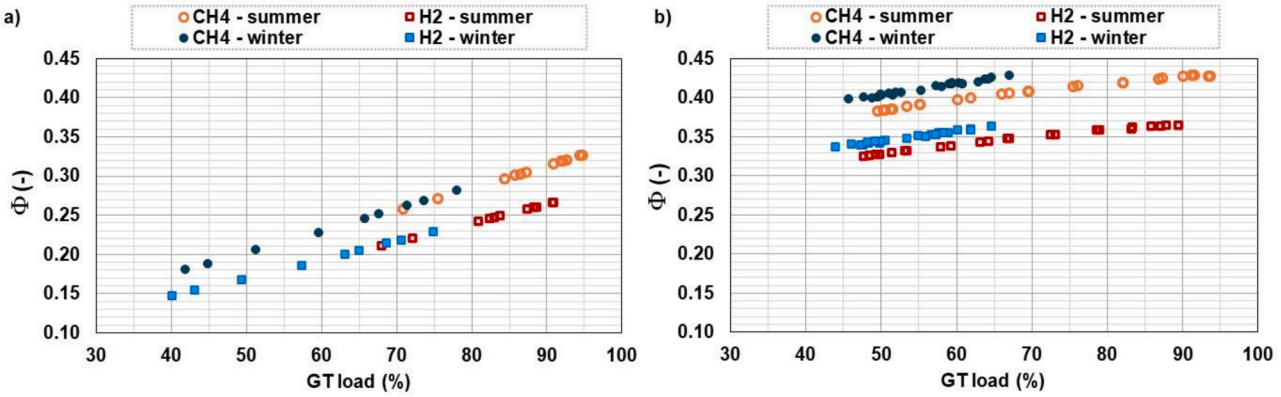

Fig. 20. Equivalence ratio of GT operated in SC (a) and CC (b) mode, in summer and winter day: NG vs. H_2.

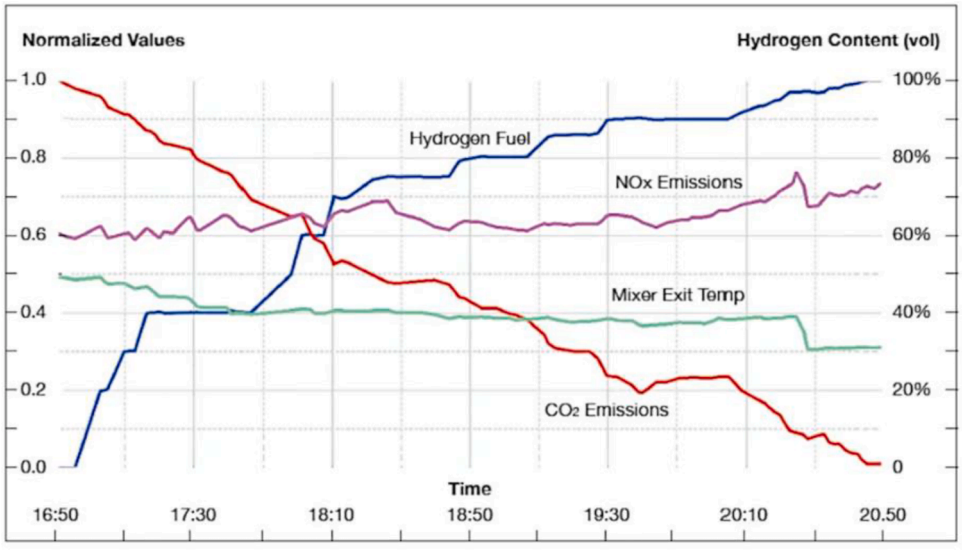

Fig. 21. Overview of GT36 single can test run at full pressure conditions (Ciani et al., 2024).

operation was proved fully possible, bringing the CO_2 emissions, measured at the combustor exit, down to zero.

3.4. Environmental impact and expected costs

Considerations on the environmental impact of the investigated systems started with the quantification of the CO_2 content in the exhaust gas when NG is used. Table 7 (top) shows that the CO_2 mol fraction is

Table 7
Overview of CO_2 emissions.

	SC mode	CC mode
CO_2 (mol %) – Fuel: NG		
Summer day	2.45–3.07	3.63–4.04
Winter day	1.75–2.69	3.79–4.06
Avoided CO_2 (kg/s) – Fuel: H_2		
Summer day	5.22–6.67	27.37–40.37
Winter day	3.98–6.38	28.96–36.66
Avoided CO_2 / H_2 fuel flow (-)	6.6–6.7	

below the threshold of 4 % due to the dilution effects caused by part load operation, which is more significant in the SC case (as explained in Section 3.3. When NG is totally replaced by hydrogen, the amount of avoided CO_2 fluctuates according to the imposed load profiles within the range reported in Table 7 (bottom). Moreover, the ratio of the avoided CO_2 emissions to the hydrogen consumption was calculated, resulting in a value of 6.6–6.7 in both cases. This coefficient could be useful as benchmarking against CO_2 production correlated to the hydrogen production process, with the aim to roughly evaluate the overall CO_2 balance.

Depending on the primary energy and production pathway, the carbon footprint of hydrogen from the well-to-consumption gate was taken from Antoni (2024). It was inferred that CO_2 emissions due to hydrogen supply by fossil fuels do not exceed the CO_2 savings of hydrogen-fueled GTs provided that carbon capture is applied, with a relatively high capture efficiency (above 90 %). This is true for either steam methane reforming or coal gasification. One potential solution to avoid CO_2 capture is the production of hydrogen from biomass. Electrolysis would be the optimal choice, provided that the electricity is derived from solar, wind, or nuclear sources.

As regards the costs associated with fully replacing NG in small and large-scale GT power plants, a rough estimate of the levelized cost of electricity (LCOE) was made relying on the research work carried out by the European Turbine Network (ETN, 2022). The key point is that the higher the level of hydrogen blending, the greater the LCOE. With 100 % hydrogen, LCOE may rise by about 85 % and 60 % in SC and CC mode, respectively, compared to NG cases (Table 8). The contribution of the hydrogen cost to LCOE is around 70–80 %, with the higher percentage in CC mode. Please note that these estimates relate to the following hypotheses: hydrogen cost of 1.5 €/kg; NG cost of 20 €/MWh; CO_2 price of 50 €/ton; GT upgrade and fixed maintenance costs increased by 25 % and 50 %, respectively, compared to the conventional fuel; annual operating hours of 800 and 6000 for SC and CC case. Clearly, increasing both η and the capacity factor can make a difference. As hydrogen production technology matures, these LCOE values are expected to decrease. Additionally, the yearly operating hours for the SC case will increase to meet growing peaking demand.

4. Conclusions

An hourly simulation method was developed to mimic the behavior of gas turbine power plants when called upon to meet the demand of the electricity grid in two different modes: peaker GT in simple cycle and load-following GT in combined cycle. The scenario took into account realistic variations in electrical load throughout a day, in winter and summer, for two representative US cities. For each GT mode, part-load control strategies were developed to boost thermal efficiency. To quantify the influence of burning hydrogen on thermodynamic performance, standard fuel (100 % CH_4) was compared to pure H_2, under the same external constraints (power to be produced and environmental conditions). The beneficial impact of H_2, compared with NG, can be outlined as follows:

- For SC GT, in which the fuel flow rate follows the electricity demand whereas the intake air only varies with the ambient conditions, the increase in η_{GT} grows linearly with GT load: it is 0.3 pp at 40 % GT load and reaches 0.6 pp at about 90 % GT load.
- For CC GT, where both fuel and airflow are varied to meet the electrical load, while rising TOT at the highest possible level (set at 50 °C above the rated value), the increase in η_{CC} is governed by TOT and thus the power sharing between the topping (Joule-Brayton) cycle and bottoming (Rankine) cycle: it covers a range between 0.44 and 0.57 pp.

Whatever the operation mode, hydrogen combustion led to leaner conditions: the overall equivalence ratio decreases from [0.18–0.33] to [0.15–0.27] in the SC case and from [0.38–0.43] to [0.32–0.36] in the CC case. These results were obtained by ensuring that TIT levels with H_2 do not exceed those with NG. The decarbonization of the exhaust was confirmed since the predicted CO_2 fraction at the stack is below 0.03 % vol on both days.

A further development of this investigation concerns the prediction of NO_x emissions, with the awareness that a more complex combustor model would be needed to handle the fuel split in the different regions/stages. Economic aspects also deserve attention given the significant involvement of GT engines in meeting the continuous growth in electricity demand.

Funding

This research did not receive any specific grant from funding agencies in the public, commercial, or not-for-profit sectors.

CRediT authorship contribution statement

Matteo Cappellini: Validation, Software, Methodology, Formal analysis. **Chiara Castagna:** Validation, Software, Methodology, Formal analysis. **Silvia Ravelli:** Writing – review & editing, Writing – original draft, Supervision, Methodology, Conceptualization.

Declaration of competing interest

The authors declare that they have no known competing financial interests or personal relationships that could have appeared to influence the work reported in this paper.

Table 8
LCOE assessment based on E.T.N., 2022.

Source: ETN, 2022	**SC mode 8**		**CC mode CC mode**	
h/year	800		6000	
	100 % NG	**100 % H_2**	**100 % NG**	**100 % H_2**
LCOE (€/MWh)	98	182	60	96

Appendix A1

This section aims to provide technical information on the numerical settings underlying the use of Thermoflex®. Sources are previous works on hydrogen feeding to GT power plants (Ravelli, 2022, 2023). A comprehensive solution was derived for each power plant component's steady-state heat and mass balances, culminating in an algebraic system of equations comprising input and output parameters, including pressure, temperature, enthalpy, and mass flow rate. The convergence tolerance was set to be within 10^{-4}, whereas the power convergence was within 0.01 %, as determined through four consecutive loops, with each loop comprising up to 300 iterations.

For the GT, compressor-turbine matching is based on the approach delineated by Bexten et al. (2021), who provided detailed equations of the so-called property factors. In short, β can be mapped out as a function of axial and tangential Mach number (M_{ax} and M_{tg}, respectively). From the continuity equation and the equation of state the following can be obtained:

$$M_{ax} \sim \frac{m\sqrt{RT}}{p\sqrt{\gamma}} \quad (1)$$

$$M_{tg} \sim \frac{n}{\sqrt{\gamma RT}} \quad (2)$$

The turbine was assumed to behave like a choked nozzle according to the following:

$$\frac{m\sqrt{RT_i}}{p_i} \sim const \quad (3)$$

In the CC case, the steam turbine shown in Fig. 4b consists of many stages. It behaves like a choked nozzle of a fixed throat area (right member) according to the following:

$$\frac{m\sqrt{T_i}}{p_i} \sim const \quad (4)$$

In off-design mode, the pressure-flow relationship in eq. (4) is used holding the nozzle area fixed. Matching all stage groups to each other requires an iterative process, since the state entering a group is affected by that exiting from its upstream neighbor. At partial load, p_i decreases with m but stage efficiency stays constant in sliding mode.

Fuel flow in the combustor undergoes fully oxidation: the energy available corresponds to its heating value. Combustion implies that fuel's consumed carbon and sulfur are fully oxidized. Other compounds, generally produced in much smaller amounts, are difficult to predict from first principles, with complex dependencies upon details of equipment beyond the scope of the software.

As regards the "control loop" algorithm, it instructs the software to adjust certain control variables in order to cause a set point parameter to attain a desired value. The schematic in Fig. A.1 shows an example of the computation for the GT in SC mode under the constraints of electrical load=19.9 MW and T_{amb}=1.1 °C (h. 16 in winter day). The control uses the successive computed values of the target (P_g) to guide further iterations in its search for the set point value, by adjusting the GT load within the defined search space .

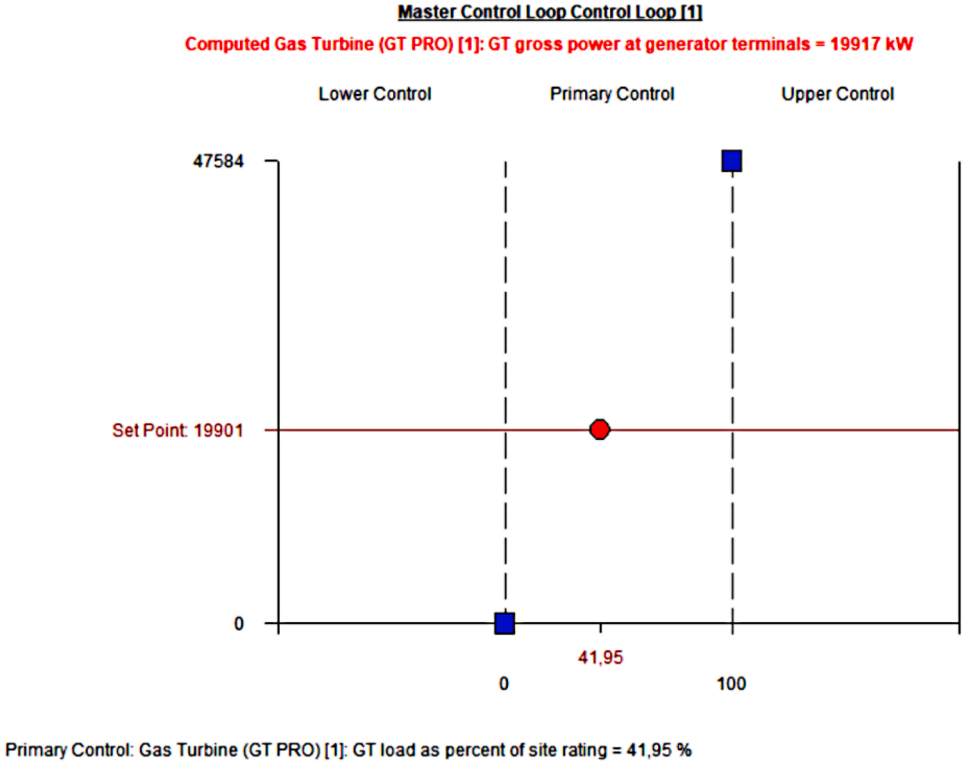

Fig. A.1. Example of main control loop output (screenshot of Thermoflex®).

Appendix A2

In order to demonstrate the validity of the simulation method applied, the source of data available from Seydel (2015) was chosen as the basis for comparison: note that the GT runs at constant TOT. Calculations for the GE 6B03 were carried out at ISO ambient conditions and full load, by varying the H_2 vol fraction from 0 to 100 %. Results are exhibited in Fig. A2a and A2c. While the air mass flow at the combustor inlet remains unchanged, the exhaust mass flow decreases due to the fuel mass flow reduction, which compensates for the higher LHV of H_2, compared to NG (Fig. A2a).

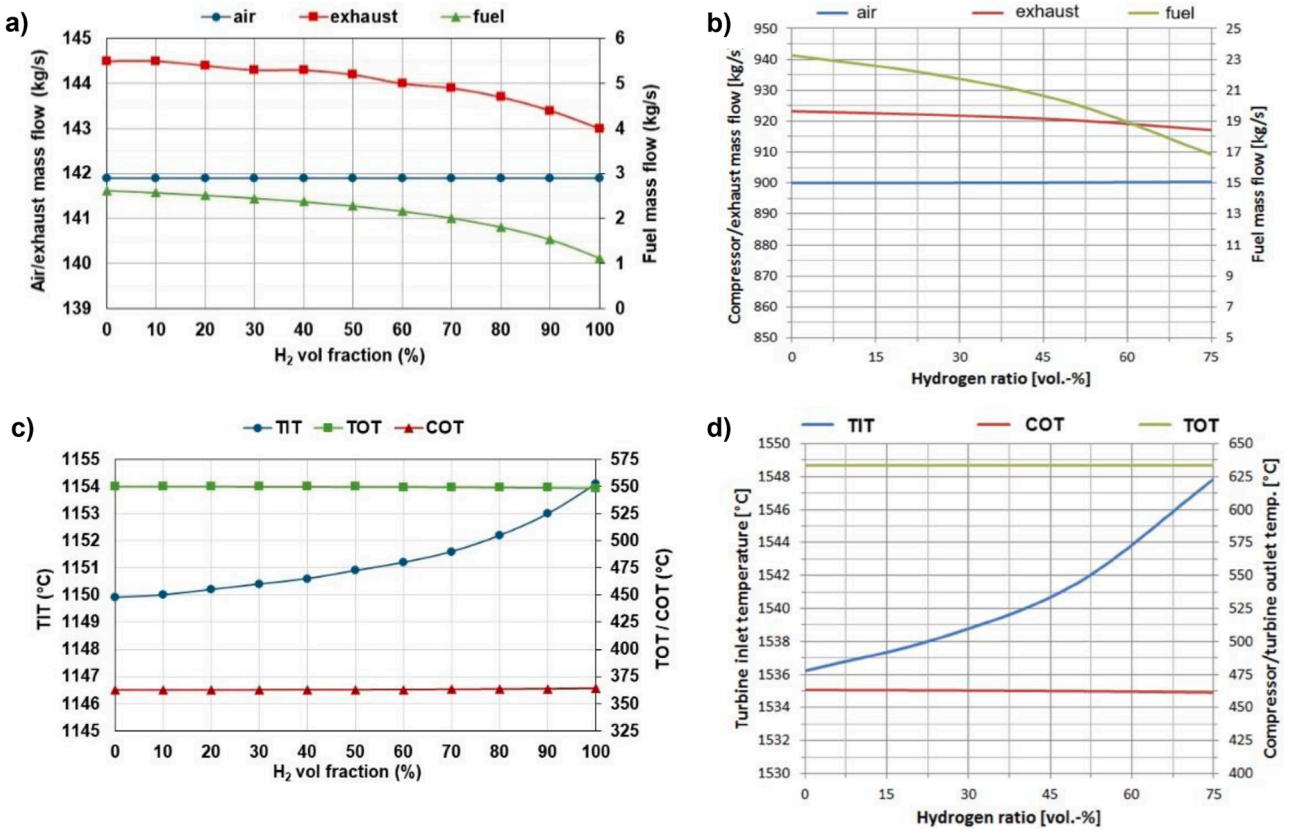

Fig. A.2. Validation of GT performance as a function of H_2 content: simulations (a, c) vs. literature data (b, d) – source: Seydel (2015).

As per the control strategy, TOT is kept constant as well as the compressor outlet temperature (COT), while TIT increases slightly with H_2 content, to comply with the choked condition of the first turbine stage (Fig. A2c). For all variables, the curves show very good agreement with those obtained by Seydel (Figs. A2b and A2d).

In addition, the method used by Jeong et al. (2024) was adopted to GE 6B03. Pure hydrogen was compared with NG keeping the same nominal GT power output (full load, ISO conditions) of 43.96 MW. As shown in Table A2, the model delivered consistent results in terms of: decrease in turbine inlet flow and temperature, as well as in exit temperature. The slight increase in η_{GT} was confirmed (0.60 vs. 0.54 pp).

Table A2
Validation of hydrogen-fueled GT in SC mode against Jeong et al. (2024).

	Jeong et al. (2024)			GE 6B03 – SC mode		
	100 % CH_4	100 % H_2	Δ (%)	100 % CH_4	100 % H_2	Δ (%)
TIT (°C)	1300	1268.1	−2.52	1149.9	1123.5	−2.35
Turbine inlet flow (kg/s)	101.35	100.05	−1.30	134.0	132.4	−1.21
TOT (°C)	569	549.3	−3.59	550.0	530.5	−3.68
η_{GT} (%)	36.20	36.74	1.47	33.54	34.14	1.76

Moreover, the author successfully exploited this approach in previous works dealing with hydrogen co-firing in a fully decarbonized CC operating in load-following mode (Ravelli, 2024).

Data availability

The authors do not have permission to share data.

References

Álvarez, J.F.G., Sahota, S., Lombardi, L., 2024. Study on fuel flexibility of a medium size gas turbine fueled by different hydrogen-based fuels from biowaste as possible alternatives to natural gas. Env. Res. 250, 118399. https://doi.org/10.1016/j.envres.2024.118399.

Amrouche, F., Boudjemaa, L., Bari, O.K., 2025. Hydrogen-natural gas blending for enhanced performance of the MS-5002C gas turbine in Southern Algeria. Int J Hydrog. Energy 106, 1144. https://doi.org/10.1016/j.ijhydene.2025.02.049.
Andrews, G.E., 2013. Ultra-low nitrogen oxides (NO_x) emissions combustion in gas turbine systems. Modern Gas Turbine Systems. Woodhead Publishing, pp. 715–790. https://doi.org/10.1533/9780857096067.3.715.
Antoni, L., 2024. Methodology for Determining the Greenhouse Gas Emissions Associated with the Production, Conditioning, and Transport of Hydrogen to Consumption Gate. Webinar. https://www.esmap.org/sites/default/files/Presentations/2024_01_23_Webinar_IPHE.pdf.
Berg, A., Magnusson, R., 2023. Fleet experience of SGT-600 (24 MW) DLE gas turbine with over 60% H_2 in natural gas. In: Proceedings of the ASME Turbo Expo 2023: Turbomachinery Technical Conference and Exposition. Volume 3B: Combustion, Fuels, and Emissions. ASME, Boston, Massachusetts, USA. https://doi.org/10.1115/GT2023-103650. V03BT04A050.
Bexten, T., Jörg, S., Petersen, N., Wirsum, M., Liu, P., Li, Z., 2021. Model-based thermodynamic analysis of a hydrogen-fired gas turbine with external exhaust gas recirculation. J. Eng. Gas. Turbine Power. 143 (8), 081016. https://doi.org/10.1115/1.4049699.
Blätte, L., Goeb, D., Gruhlke, P., Prade, B., Schildmacher, K., Streb, H., Vogtmann, D., 2024. SGT5-4000F Hydrogen capability - high pressure combustion rig tests part II. In: Proceedings of the ASME Turbo Expo 2024: Turbomachinery Technical Conference and Exposition. Volume 3A: Combustion, Fuels, and Emissions. ASME, London, United Kingdom. https://doi.org/10.1115/GT2024-123364. V03AT04A023.
Blaette, L., Schmitz, U., Streb, H., Vogtmann, D., 2023. SGT5-4000F Hydrogen capability – High pressure combustion rig tests. In: Proceedings of the ASME Turbo Expo 2023: Turbomachinery Technical Conference and Exposition. Volume 3B: Combustion, Fuels, and Emissions. ASME, Boston, Massachusetts, USA. https://doi.org/10.1115/GT2023-103574. V03BT04A046.
Cecere, D., Giacomazzi, E., Di Nardo, A., Calchetti, G., 2023. Gas turbine combustion technologies for hydrogen blends. Energies 16 (19), 6829. https://doi.org/10.3390/en16196829.
Chiesa, P., Lozza, G., Mazzocchi, L., 2005. Using hydrogen as gas turbine fuel. ASME. J. Eng. Gas Turbines Power 127 (1), 73–80. https://doi.org/10.1115/1.1787513.
Ciani, A., Sanchez, P.S., Wickström, A., Pennell, D., Stefanis, V., Früchtel, G., 2024. Ansaldo Tests 100% Hydrogen Fuel Using Sequential Combustion. https://gasturbineworld.com/sequential-combustion-technology-tested-100-percent-hydrogen/.
Demougeot, N., Bullard, T., Kalb, B., Hernandez, F., Spalding, M., Yaquinto, M., Soffritti, G., van den Hout, F., Lee, D.K., Hwang, J.W., 2024. Heavy duty H_2 gas turbine demonstration – A combined experience. In: Proceedings of the ASME Turbo Expo 2024: Turbomachinery Technical Conference and Exposition. Volume 6: Education; Electric Power; Energy Storage; Fans and Blowers. ASME, London, United Kingdom. https://doi.org/10.1115/GT2024-126848. V006T08A008.
EIA, U.S. Energy Information Administration, 2023. Hourly Electric Grid Monitor, https://www.eia.gov/electricity/gridmonitor/dashboard/electric_overview/US48/US48.
Elmasri, M.A., 2009. Design of Gas Turbine Combined Cycles and Cogeneration Systems. Thermoflow Inc, Jacksonville, FL.
EUTurbines, 2021. H2-Readiness of Turbine Based Power Plants – A Common Definition. https://www.euturbines.eu/wp-content/uploads/2021/09/EUTurbines-H2-ready-Definition-September-2021-1.pdf.
Gazzani, M., Chiesa, P., Martelli, E., Sigali, S., Brunetti, I., 2014. Using hydrogen as gas turbine fuel: premixed versus diffusive flame combustors. ASME. J. Eng. Gas Turbines Power 136 (5), 051504. https://doi.org/10.1115/1.4026085.
GE, 2021. 6 B HEAVY DUTY GAS TURBINE, https://www.gevernova.com/content/dam/gepower-new/global/en_US/downloads/gas-new-site/products/gas-turbines/6b-fact-sheet-product-specifications.pdf.
Giacomazzi, E., 2013. The importance of operational flexibility in gas turbine power plants. EAI Energ. Ambiente Innov. 6, 58–63. https://doi.org/10.12910/EAI2013-35.
Harper, J., Cloyd, S., Pigon, T., Thomas, B., Wilson, J., Johnson, E., Noble, D.R., 2023. Hydrogen Co-firing demonstration at Georgia Power's plant McDonough: M501G gas turbine. In: Proceedings of the ASME Turbo Expo 2023: Turbomachinery Technical Conference and Exposition. Volume 6: Education; Electric Power; Energy Storage; Fans and Blowers. ASME, Boston, Massachusetts, USA. https://doi.org/10.1115/GT2023-102660. V006T08A007.
Harper, J., Gibeaut, D., Lozier, M., Sake, R., Wolf, T., Noble, D.R., 2025. Hydrogen cofiring demonstration at Constellation Hillabee Siemens Energy SGT6-6000G power plant. ASME. J. Eng. Gas Turbines Power 147 (5), 051025. https://doi.org/10.1115/1.4067181.
Horikawa, A., Ashikaga, M., Yamaguchi, M., Ogino, T., Aoki, S., Wirsum, M., Funke, H. H., Kusterer, K., 2022. Combined heat and power supply demonstration of Micro-mix hydrogen combustion applied to M1A-17 gas turbine. In: Proceedings of the ASME Turbo Expo 2022: Turbomachinery Technical Conference and Exposition. Volume 3A: Combustion, Fuels, and Emissions. ASME, Rotterdam, Netherlands. https://doi.org/10.1115/GT2022-81620. V03AT04A041.
IEA, 2023. Global Hydrogen Review 2023, Paris. https://www.iea.org/reports/global-hydrogen-review-2023. Licence: CC BY 4.0.
IEA, 2024. Global Hydrogen Review 2024, Paris. https://www.iea.org/reports/global-hydrogen-review-2024. Licence: CC BY 4.0.
IEA, 2025. Electricity 2025, Paris. https://www.iea.org/reports/electricity-2025. Licence: CC BY 4.0.
Jansohn, P., 2013. Modern Gas Turbine Systems: High Efficiency, Low Emission, Fuel Flexible Power Generation. Series in Energy, ISSN: 2044-9364.
Jeong, J.H., Park, H.S., Park, Y.K., & Kim, T.S., 2024. Analysis of the influence of hydrogen co-firing on the operation and performance of the gas turbine and combined cycle. Case Stud. Therm. Eng. 54, 104061. https://doi.org/10.1016/j.csite.2024.104061.
Kapoor, R., Bullard, T., Shoraka, A., Hsia, K.T., 2024. Impact of hydrogen fuel retrofits to gas turbine performance and hot gas path components. In: Proceedings of the ASME Turbo Expo 2024: Turbomachinery Technical Conference and Exposition. Volume 6: Education; Electric Power; Energy Storage; Fans and Blowers. ASME, London, United Kingdom. https://doi.org/10.1115/GT2024-126838. V006T08A007.
Koç, Y., Yağlı, H., Görgülü, A., Koç, A., 2020. Analysing the performance, fuel cost and emission parameters of the 50 MW simple and recuperative gas turbine cycles using natural gas and hydrogen as fuel. Int. J. Hydrog. Energy 45 (41), 22138. https://doi.org/10.1016/j.ijhydene.2020.05.267.
Kytömaa, H., Wechsung, A., Dimitrakopoulos, G., Cook, N., Jaimes, D., Hur, I.Y., Faraji, S., 2024. Industry R&D needs in hydrogen safety. Appl. Energy Combust. Sci. 18, 100271. https://doi.org/10.1016/j.jaecs.2024.100271.
Laget, H., Griebel, P., Gooren, L., Hampp, F., Jouret, N., Lammel, O., 2022. Demonstration of natural gas and hydrogen Co-combustion in an industrial gas turbine. In: Proceedings of the ASME Turbo Expo 2022: Turbomachinery Technical Conference and Exposition. Volume 2: Coal, Biomass, Hydrogen, and Alternative Fuels; Controls, Diagnostics, and Instrumentation; Steam Turbine. ASME, Rotterdam, Netherlands. https://doi.org/10.1115/GT2022-80924. V002T03A007.
Moliere, M., Hugonnet, N., GE Energy, 2004. Hydrogen-fueled gas turbines: experience and prospects. In: Proceedings of the Power-Gen Asia 2004. Bangkok, 5-7 October 2004.
Morales, M.J.M., Blondeau, J., De Paepe, W., 2024. Assessing the impact of CH_4/H_2 blends on the thermodynamic performance of aero-derivative gas turbine CHP configurations. Int. J. Hydrog. Energy 67, 159–171. https://doi.org/10.1016/j.ijhydene.2024.04.137.
Munther, H., Hassan, Q., Mohammed, A., Hanoon, T.M., Algburi, S., 2025. Techno-economic and environmental evaluation of green hydrogen Co-firing in a 570 MWe gas turbine combined cycle power plant in Iraq. Unconv. Resour. 6, 100163. https://doi.org/10.1016/j.uncres.2025.100163.
Mustafa, L., Ślefarski, R., Jankowski, R., 2024. Thermodynamic analysis of gas turbine systems fueled by a CH_4/H_2 mixture. Sustainability. 16 (2), 531. https://doi.org/10.3390/su16020531.
NETL, 2022. A literature review of hydrogen and natural gas turbines: current State of the art with regard to performance and NOx control, DOE/NETL-2022/3812. https://netl.doe.gov/sites/default/files/publication/A-Literature-Review-of-Hydrogen-and-Natural-Gas-Turbines-081222.pdf.
European Turbine Network (ETN), Global, 2022. Hydrogen Deployment in Centralised Power Generation A Techno-Economic Case Study. ETN a.i.s.b.l., Brussels, Belgium.
Neville, 2023. The future of hydrogen as a gas turbine fuel. Turbomach. Mag. 64 (4). https://www.turbomachinerymag.com/view/the-future-of-hydrogen-as-a-gas-turbine-fuel.
Öberg, S., Odenberger, M., Johnsson, F., 2022. The value of flexible fuel mixing in hydrogen-fueled gas turbines–a techno-economic study. Int. J. Hydrog. Energy 47 (74), 31684. https://doi.org/10.1016/j.ijhydene.2022.07.075.
Parsania, N., Hermeth, S., Witzel, B., Yilmaz, E., Fourcade, S., Garmadi, S., Trump, H., McCaig, P., 2024. HYFLEXPOWER Project: demonstration of an industrial power-to-H_2-to-power advanced plant concept with up to 100% H_2 in an SGT-400 gas turbine. In: Proceedings of the ASME Turbo Expo 2024: Turbomachinery Technical Conference and Exposition. Volume 2: Ceramics and Ceramic Composites; Coal, Biomass, Hydrogen, and Alternative Fuels. ASME, London, United Kingdom. https://doi.org/10.1115/GT2024-124016. V002T03A013.
Pennell, D., Tay-Wo-Chong, L., Smith, R., Sierra Sanchez, P., Ciani, A., June 26–30, 2023. GT36 First stage development enabling load and fuel (H2) flexibility with low emissions. In: Proceedings of the ASME Turbo Expo 2023: Turbomachinery Technical Conference and Exposition. Volume 3B: Combustion, Fuels, and Emissions. Boston, Massachusetts, USA. ASME. https://doi.org/10.1115/GT2023-103568. V03BT04A045.
Pigon, T., Cloyd, S., Springer, C., Boggs, J., Shiraiwa, T., Yamazaki, S., 2023. Best practices from Hydrogen fuel system retrofit. In: Proceedings of the ASME Turbo Expo 2023: Turbomachinery Technical Conference and Exposition. Volume 2: Ceramics and Ceramic Composites; Coal, Biomass, Hydrogen, and Alternative Fuels. ASME, Boston, Massachusetts, USA. https://doi.org/10.1115/GT2023-101368. V002T03A006.
Ravelli, S., 2022. Thermodynamic assessment of exhaust gas recirculation in high-volume hydrogen gas turbines in combined cycle mode. J. Eng. Gas. Turbine Power. 144 (11), 111012. https://doi.org/10.1115/1.4055353.
Ravelli, S., 2023. Reducing the energy penalty of retrofit decarbonization in combined cycle power plants. J. Eng. Gas. Turbine Power. 145 (12), 121003. https://doi.org/10.1115/1.4063317.
Ravelli, S., 2024. Thermodynamic optimization of load-following operation in a decarbonized combined cycle power plant under net-zero scenarios. J. Eng. Gas. Turbine Power. 146 (10), 101020. https://doi.org/10.1115/1.4065920.
Seydel, C.G., 2015. Performance influences of hydrogen enriched fuel on heavy-duty gas turbines in combined cycle power plants. In: Proceedings of the ASME Turbo Expo 2015: Turbine Technical Conference and Exposition. Volume 3: Coal, Biomass and Alternative Fuels; Cycle Innovations; Electric Power; Industrial and Cogeneration. ASME, Montreal, Quebec, Canada. https://doi.org/10.1115/GT2015-42018. V003T08A002.
Shilling, N., Z, PE, D., 2023. Emissions and Performance Implications of Hydrogen Fuel in Heavy Duty Gas Turbines. Clean Air Task Force.
Siemens Energy. SGT5-4000F gas Turbine, https://www.siemens-energy.com/global/en/home/products-services/product/sgt5-4000f.html#/.

Skabelund, B.B., Jenkins, C.D., Stechel, E.B., Milcarek, R.J., 2023. Thermodynamic and emission analysis of a hydrogen/methane fueled gas turbine. Energy Convers. Manag.: X 19, 100394. https://doi.org/10.1016/j.ecmx.2023.100394.

Steele, R.C., Martz, T.D., Ettlinger, A., Zandes, T., Alexander, M.J., Hockman, B.K., Goldmeer, J., 2023. Hydrogen Co-firing demonstration at New York Power Authority Brentwood site: GE LM6000 gas turbine. In: Proceedings of the ASME Turbo Expo 2023: Turbomachinery Technical Conference and Exposition. Volume 6: Education; Electric Power; Energy Storage; Fans and Blowers. ASME, Boston, Massachusetts, USA. https://doi.org/10.1115/GT2023-101283. V006T08A001.

Stefan, E., Talic, B., Larring, Y., Gruber, A., Peters, T.A., 2022. Materials challenges in hydrogen-fuelled gas turbines. Int. Mater. Rev. 67 (5), 461–486. https://doi.org/10.1080/09506608.2021.1981706.

Weather Spark, 2023. https://weatherspark.com/.

Zhou, H., Xue, J., Gao, H., Ma, N., 2024. Hydrogen-fueled gas turbines in future energy system. Int. J. Hydrog. Energy 64, 569–582. https://doi.org/10.1016/j.ijhydene.2024.03.327.